

# Smelting Experiments with Chalcopyrite Ore based on Evidence from the Eastern Alps

*Thomas Rose, Erica Hanning and Sabine Klein*

## Keywords

Copper, roasting, smelting experiments, XRD, Mitterberg

## Abstract

In order to assess the fractionation of copper isotopes during smelting under reconstructed conditions, smelting experiments with chalcopyrite ore were conducted in built furnaces based on archaeometallurgical evidence from the Bronze Age Eastern Alps and ethnographic examples from Nepal. Two experimental series, S2 and S4 were chosen for analysis. Each series consisted of a number of roasting and smelting experiments with different experimental parameters, and both series yielded metallic copper. Each type of experiment, their outcomes, and observations made during them are described in detail to facilitate future experimental work. Both series differ significantly in their outcome. XRD analyses and chemical analyses were carried out to reveal the reasons for the observed differences. The chemistry of the obtained matte shows that roasting is pivotal for a successful smelting process and that two cycles of matte roasting and subsequent smelting can be sufficient to remove most of the sulphur and iron from the matte. Furthermore, different conditions in the shaft furnaces resulted in a more efficient oxidation of iron in series S4. During the subsequent smelting of the matte in the pit furnace, it was possible to extract larger amounts of metallic copper and sponge copper, as well as to produce a thin well-melted plate-like slag. The pit furnace did not always show clear traces of metallurgical activity and thus might not be identifiable in the archaeological records without chemical analysis of the pit lining and surrounding soil. Although more trials are needed to replicate the process, these experiments give a strong hint towards the reconstruction of the matte smelting process in the Bronze Age alpine area.

## Introduction

Isotope studies have become quite routine on archaeological materials. For example, the geochronological in-

formation gained by lead isotope analysis is commonly used to connect metal artefacts to their ore source, due to the fact that the four relatively heavy lead isotopes do not significantly fractionate during smelting and melting, and the isotope signature variation within an ore body is usually smaller than the variation between different occurrences (see Klein, 2007).

The two copper isotopes,  $^{65}\text{Cu}$  and  $^{63}\text{Cu}$ , on the other hand, are sensitive to oxidizing and reducing conditions, and do indeed fractionate near the surface of the ore body through solution effects influenced by meteoric water (Mathur and Fantle, 2015). This means that surface-near fluids and copper ores in the supergene enrichment zones are enriched in  $^{65}\text{Cu}$ , while the copper ores in the oxidation zone are depleted in  $^{65}\text{Cu}$ . The unweathered primary ore body does not exhibit significant fractionation (Asael, et al., 2007; 2012). The copper isotope ratios thus can be used as potential redox-markers, giving evidence for the use of surface-near secondary oxide ores or deeper supergene and primary sulphide ore minerals (Asael, et al., 2009; 2012; Mathur and Fantle, 2015), and subsequently mirroring the particular technical abilities and exploitation history of mines or mining areas (Klein, et al., 2010). Copper isotope ratios in archaeological artefacts have also been used to argue a shift in copper smelting technology and ensuing temporal gap in copper production as the smelters had to contend with the more difficult smelting process of copper sulphides (see discussion in Jansen, 2018; Powell, et al., 2017; Powell, et al., 2018).

However, what was still lacking for the archaeometallurgical understanding of the copper isotope system is how the copper isotopes behave during smelting of the copper ore. A first attempt was made in small studies investigating copper isotope fractionation during crucible smelting of an oxide ore. The experiments were carried out under controlled conditions and with

a pure starting material (Bower, et al., 2013; Gale, et al., 1999; Rose, et al., 2017).

At this point, it was deemed necessary to test the fractionation of copper isotopes under more authentic archaeological conditions in furnaces, which were reconstructed based on Bronze Age furnace remains, and using pieces of sulphide copper ore collected from ancient mining sites. Remains of copper metallurgy founded on the smelting of sulphide ore have been studied in depth from many different sites around the world and throughout all relevant archaeological time periods. In the present study, the example chosen for the reconstruction is from the Mitterberg area (St. Johann im Pongau, Austria) with its numerous copper smelting sites, as well as mines and ore beneficiation sites, making it one of the most important copper production areas during the Alpine Bronze Age (see Stöllner, 2011; Stöllner, Hanning and Hornschuch, 2011). The reason for this reconstruction choice is that there is clear archaeological evidence of roasting beds, which indicates a separate oxidizing step of the sulphide ore (e.g. Zschocke and Preuschen, 1932, Czedik-Eisenberg, 1958), as well as previous experience of one of the authors in reconstructing this process (Hanning and Pils, 2011; Hanning, 2012; Goldenberg, et al., 2011).

In the present contribution, the experiments, materials, and installations are presented in detail to facilitate future smelting experiments. XRD analyses on selected samples and chemical analyses were also carried out. The observations made during the smelting experiments, the smelting products obtained, the XRD data and the chemical composition of the matte are used to evaluate the experiments and their outcomes and to identify potential approaches for future experiments. Moreover, all smelting experiments described here, their data sheets (Rose, Klein and Hanning, 2020), and their smelting products serve as material base for the overall aim of our project: The identification of copper isotope fractionation occurring during smelting of copper ores (Klein and Rose, 2020).

## Smelting of copper sulphide ores

While copper carbonates such as malachite or azurite, can be relatively easily smelted in a reducing atmosphere, which can be achieved e. g. in a charcoal covered pit, the smelting of copper sulphides requires additional steps before metal can be obtained. In the experiments presented here, chalcopyrite ore was used, which requires the removal of the sulphur and iron bound to the copper. Usually this separation is achieved through

a combination of repeated roasting and smelting of the ore (Figure 1).

During roasting, the crushed ore is heated to relatively low temperatures (600 to 900 °C) in an open fire. In a solid-state reaction, the sulphur in the ore reacts with the oxygen to form gaseous sulphur dioxide, and the iron and copper are converted to oxides. The oxidation must be done without sintering or even liquefying the ore pieces in order to prevent reduction of particle surface–oxygen contact area (Shamsuddin, 2016, p.42). When the sulphur is completely removed and the iron and copper has been converted to oxides – a so-called dead roast – the roasted ore can be converted to metal in a reducing atmosphere (Bachmann, 1993; Lechtman and Klein, 1999). However, a complete roasting of the ore is nearly impossible when working under reconstructed prehistoric conditions, especially if the ore pieces are several millimetres to centimetres in size: as the size of the pieces increases, the diffusion of oxygen into the interior of the ore is impeded, leading to a stagnation of the oxidation process (Burger, et al., 2011). Moreover, a dead roast is also not desirable due to the risk of reducing the iron oxides to iron metal, creating a unusable copper-iron alloy (Czedik-Eisenberg 1958; Bachmann, 1993).

More often, the ore was only partially roasted, where a crust of oxides is formed around a sulphide-rich core (Burger, et al., 2011). Due to the higher affinity of sulphur to copper, and iron having more affinity for oxygen than for sulphur, the iron tends to be selectively oxidized during the partial roasting of chalcopyrite. Consequently partially roasted ore pieces consist of a mixture of copper and iron sulphides in their interior and a mixture of iron oxides and copper sulphides in their exterior areas (Figure 2, d).

In the next step, the roasted ore is heated to more than 900 °C. At these temperatures it begins to melt and produces a mixture of copper and iron sulphides, the matte. The iron oxides react with silica-rich material from the gangue or flux to form slag. In the end, the matte will be enriched in copper and depleted in sulphur and iron when compared to the ore. Through multiple repetitions of roasting and smelting, more sulphur and iron are removed from the smelt. While molten, slag, matte and metallic copper will separate because of their different densities, with the copper (if present) at the bottom of the furnace, the matte on top of it and the slag as the uppermost layer.

The matte can be converted to metallic copper in several different ways: (1) the sulphur and iron are completely removed through repeated roasting and smelting and the remaining copper oxides are converted to metal under reducing conditions (see above). (2) Through

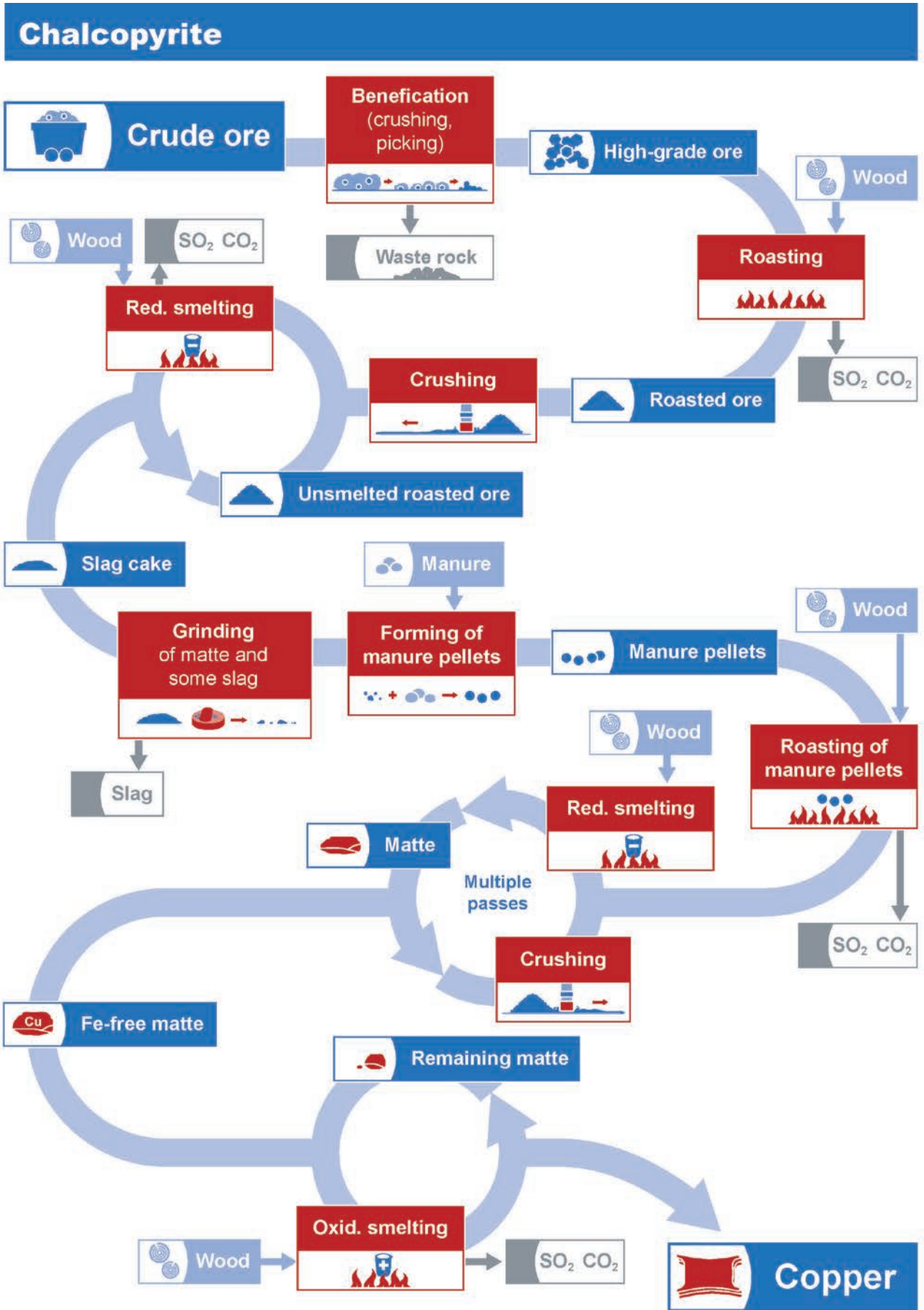


Figure 1. Schematic representation of the chalcopyrite smelting carried out in the experiments (modified after Rose, Hanning and Klein, 2019).

co-smelting – during this reaction, copper oxides formed during the roasting process react with remaining copper sulphides to form metallic copper and sulphur dioxide. (3) Taking advantage of a miscibility gap in the Cu-Fe-S system – removal of most of the iron and sulphur shifts the chemical composition of the matte so that it becomes oversaturated in copper. The copper precipitates out of the solution (as prills, which sink to the furnace bottom) leaving strongly copper-depleted matte behind (Czedik-Eisenberg, 1958; Moesta and Schnau, 1983).

## The experimental reconstruction

The installations used for the roasting of the ore and smelting it to matte were reconstructed according to the archaeological evidences dating to the Middle to Late Bronze Age in the eastern Alps<sup>1</sup>. A typical east-alpine copper smelting site consisted of three parts: roasting beds, furnaces, and slag heaps (cf. Hanning, Herdits and Silvestri, 2015). Additionally, pits of various size and shape with unclear function but with signs of being subjected to higher temperatures have also been found at these sites (Herdits and Löcker, 2004; e. g. Zschocke and Preuschen, 1932). Hence, they might have also been used in the metallurgical process.

The presence of roasting beds and furnaces indicates a (at least) two-step process comprising of oxidative roasting at low temperatures in an open fire and smelting at high temperatures in low-rise shaft furnaces. The roasting beds were rectangular, lined with clay, and surrounded by a row of stones. Their layout remained nearly unchanged until modern times (cf. Agricola, 1556 [2006]).

The reconstruction of the furnaces is more difficult because none of them have been completely preserved. Most often, the upper portion of the furnaces has been eroded away and the front wall is either completely missing or only preserved as a small lip. Most likely the front wall had to be torn down to take the smelting products out of the furnace. Fragments of funnel-shaped tuyères give evidence of the use of artificial draft, such as simple bag bellows. The circumstance that the furnaces were dug into the slope implies that the opening for the tuyères was most likely in the front wall of the furnace.

Wood analyses on material from smelting sites showed that the surrounding forests, mostly mixed coniferous forest, were exploited for fuel (Heiss and Oegg, 2008; Nelle and Klemm, 2010; Schibler, et al., 2011). Both, experiments (Fasnacht, 2010; Hanning, 2012) and historical records (Morgan, 1867; Pliny, 34:20) indicate the possibility that dried wood can be used instead of charcoal in the smelting process.

Metallic copper was rarely found at the smelting sites, but the bottoms of the plano-convex copper ingots found off-site do not fit the shape of the furnace floor. For these reasons, the production of the copper ingots directly in the furnaces is regarded as unlikely (Herdits and Löcker, 2004). It is more likely that the furnaces were used for production of the copper matte; in a further step copper was probably produced from the matte in a small refining hearth or pit furnace. Archaeological evidences of pit furnaces are easily overlooked or misinterpreted during excavation, since all that remains is a depression with traces of heating, similar to cooking pits (for further discussion of the archaeological evidence: Hanning, Herdits and Silvestri, 2015; Herdits and Löcker, 2004; Zschocke and Preuschen, 1932).

Since there is little physical evidence of the process used to refine the matte into copper metal in the Bronze Age Alps, a pit furnace similar to the one from traditional copper smelting in Nepal was used (Anfinset, 2011; Goldenberg, et al., 2011).

## Smelting experiments

### Raw materials and special equipment

The experiments were carried out on the premises of the Römisch Germanisches-Zentralmuseum (RGZM), Laboratory for Experimental Archaeology (LEA), in Mayen (Germany). Preparations for the experiments began in April 2018 with the construction of the shaft furnaces and roasting bed. The ore was roasted in April and a first smelt in the furnace (S1) was carried out in June. Most of the other experiments were carried out during four weeks in August 2018. In these weeks, among others, three experiments with the shaft furnace (S2 to S4) and several experiments with the pit furnace were carried out. Experiments with the clay crucible took place in September 2018.

The ore used (Figure 2, c) was chalcopyrite collected from the Mitterberg mining district (St. Johann im Pongau, Austria)<sup>2</sup>. The hydrothermal ore is hosted in phyllite and consists of chalcopyrite and pyrite as ore minerals with quartz, feldspar and calcite in the gangue (for the mineralogy of the Mitterberg ore veins see Bernhard, 1965).

For all experiments a mix of local coniferous wood was used except for the roasting of the ore, where deciduous wood (beech) was used. The charcoal used in the pit furnace experiments was acquired from a local charcoal maker in Kirsbach (Germany) and was produced from beech wood.

To avoid any uncontrolled contamination of the furnace charge with foreign sources of copper, the furnace



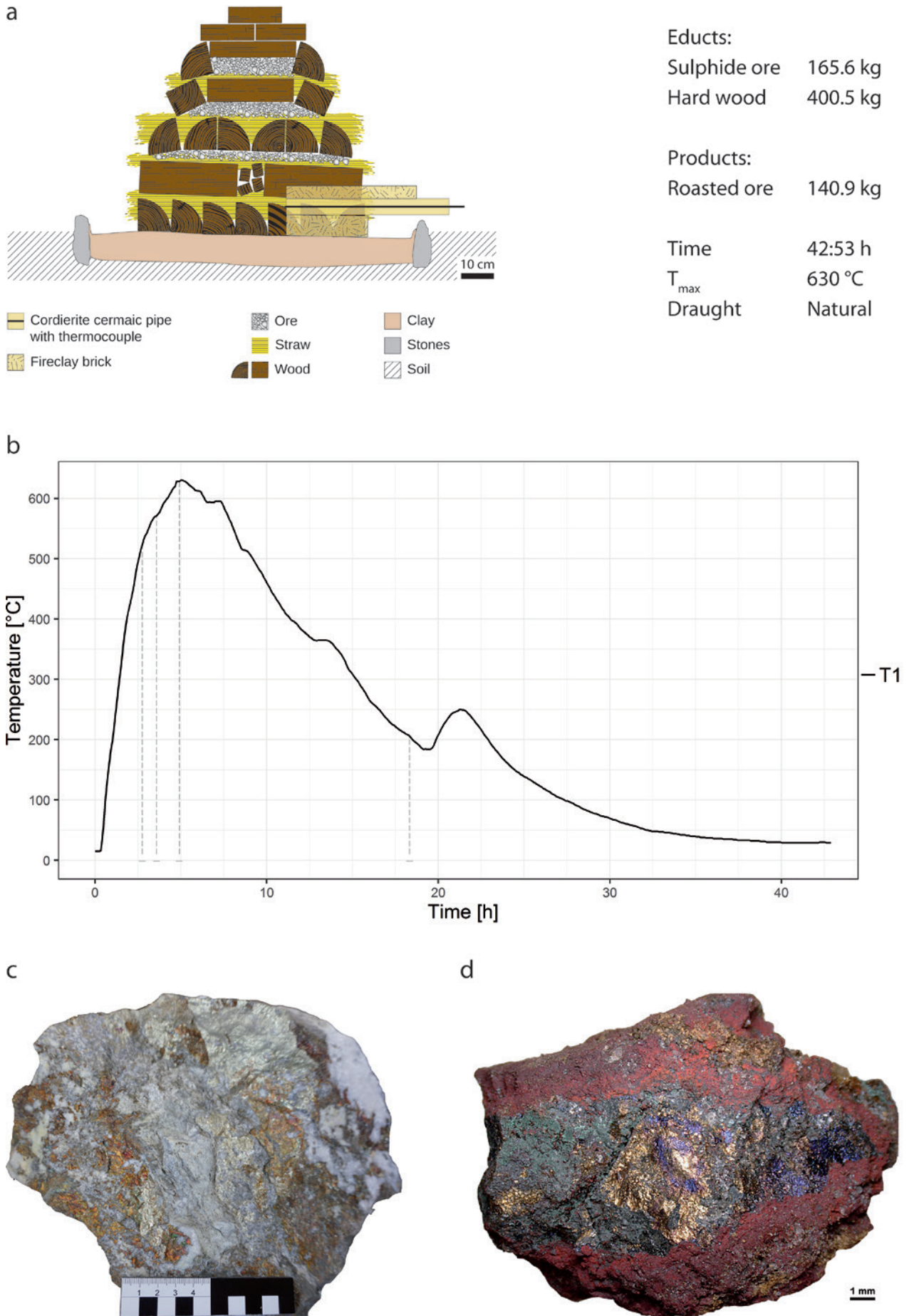


Figure 2. Roasting of the crushed ore, a) sketch of the roasting pile; b) temperature curve; c) piece of the chalcopyrite ore; d) opened piece of the roasted ore (modified after Rose, Hanning and Klein, 2019).

walls were constructed from fire bricks and coated with clay, both with a known and homogeneous composition. The same clay mixture was used throughout the experiments, not only for the furnace, but also for the lining of the roasting bed, the pit furnace and the crucibles. It was made from a mixture of 50 wt. % loam T8007, 10 wt. % clay T7012, and 40 wt. % grog temper 22/24 K, all purchased from KTS Kärlicher Ton- und Schamottewerke, Kärlich (Germany). They were thoroughly mixed with ~ 1 wt. % of flax chaff. Water was constantly added and the masse kneaded until it became a homogenous plastic mass.

For grinding and crushing the products of the smelt, suitable basalt fragments were collected from the nearby basalt quarry. For the crushing of the roasted ore and the smelting products, metal hammers were used along with hammer stones, depending on the individual preference of each participant. Deviating from this grinding setup, the unroasted ore was entirely crushed with metal hammers on tree stumps. The grinding tools were not previously used to process copper or copper ore, and hammer heads were thoroughly cleaned prior to their use in order to keep foreign contamination to a minimum.

Thermocouples of type S (Pt/10 % Rh-Pt, calibrated maximum temperature: 1500 °C, error tolerances: 1.5 K or 0.25 %) with a length of 100 cm and 60 cm were used to measure the temperature during the experiments. Alumina ceramic protection tubes (Type C799, maximum temperature 1800 °C) shielded the thermocouples from direct contact with the melt. To mount the thermocouples and to prevent them from accidental damaging during the experiments, they were placed inside a cordierite tube and the space between pipe and thermocouple filled with glass wool at both ends of the pipe. Care was taken that the tip of the thermocouple extended about 5 mm out of the cordierite tube. The thermocouples were plugged into a multi-channel data logger (PCE-T 1200). Temperatures were automatically recorded by the data logger every 60 s, and every 300 s during the roasting of the ore.

The hand-operated bag bellows were designed after ethnographic examples and had a base of ~ 60 x 35 cm<sup>2</sup> and a height of around 90 cm. Their upper openings, which act as the inlet valve, were reinforced by wooden sticks and a handle was attached on each side to allow an easy opening and closing by hand. The blast from the bellows varied greatly due to the experience and technique of the person operating the bellows, and due to the heat and occasional blow-back from the furnace, it was not possible to directly measure the airflow from the bellows into the furnace. However the airflow of the bellows was recorded in the lab using an anemometer (Tro-

tec BA06). When using an easy pace of 30 pumps per minute (1 “pump” is equal to one upward movement to fill the bellow and one downward movement to express the air through the tuyère), the blast peaked between 8 to 11 m/s, with a pause in the blast when the bellow sack was refilled with air. When working with a faster rhythm of 40 pumps per minute and pressing harder on the bellows, an intermittent blast of 16 to 18 m/s could be produced. Theoretically, then two such bellows working in an alternating rhythm would provide a blast between 10 m/s (30 pumps per minute) and 17 m/s (40 pumps per minute). This, however, is only a rough estimate, since this does not take into account that the air flow is partially blown back out of the furnace from obstructions in front of the tuyères and will also vary depending on the bellow operator(s) and asynchrony in their rhythms. Additionally, air is drawn naturally into the furnace, through gaps in the front wall and between the tuyères via the chimney effect.

The tuyères were based on archaeological examples from alpine smelting sites (e.g. Töchterle, et al., 2013). In all experiments, two tuyères were used per bellow. One tuyère was attached directly to the bellow with a leather cord and a second tuyère was inserted into the opening of the furnace or into the coals of the pits. The tuyères were fitted into each other with a small gap between them so in case hot air was blown back from the furnace, it could escape between the gap in the tuyères and did not damage the bellow. Only the ends of the tuyères which were inserted into the furnace opening became heavily slagged during the shaft furnace experiments, because they were in direct contact with the melt. As a consequence, new tuyères were used for each shaft furnace experiment to avoid contamination between the ore charges. For some pit furnace experiments, the tuyères of the same general shape but with angled nozzles were used, which more closely resembled the tuyères used by the Nepalese smelters (Anfinset, 2011). The angled tuyères helped to direct the blast of air from the pit rim down into the charcoal bed.

## Roasting of the ore

The roasting bed was constructed in a level 2 x 1 m<sup>2</sup> area, which was slightly dug into the ground and surrounded by upright standing stones of 20 to 30 cm height. The interior was lined with a 10 cm thick layer of the above-mentioned clay mixture to create a smooth unbroken surface (Figure 2, a). To record the temperature, a thermocouple was placed at the centre of the roasting bed approximately 10 cm above the clay lining. About 165 kg of ore were roasted. The aim of the experiment was to

heat the ore sufficiently to achieve a self-sustaining roasting reaction due to the exothermic reaction of sulphur to sulphur dioxide. At the same time, both the ore in the interior of the roasting pile and at the surface should be roasted uniformly, which necessitates a constant inflow of air into the centre of the roasting pile.

For these reasons the roasting pile was constructed as shown in Figure 2, a: the lower wood layers consisted of large logs, while the upper wood layers were built with smaller logs. In contrast to all other experiments, hardwood (beech) was used as fuel. To prevent the ore from falling through the logs, a layer of straw was placed between logs and ore. The uppermost straw layer was dampened to bind the ore dust.

Fire was set in one corner of the roasting pile. After ~ 1.5 hours the entire roasting pile was on fire. Ore pieces which fell from the pile due to the burning logs shifting positions were placed back in the glowing pile with a shovel. To keep the roasting reaction alive over a longer amount of time, additional wood was added several times on top of the pile (Figure 2, b). In total, 400 kg of wood were used and temperatures of up to 630 °C were recorded by the thermocouple. Yellow smoke and a very intense smell of sulphur were noticed from the very beginning. The smell was particularly strong even when flames were no longer visible.

About 43 hours after the fire was set and ~ 24 hours after the last wood was added, the roasting pile was dismantled. Glowing charcoal was not observed on the surface of the roasting pile but from some spots, sulphuric fumes were still rising, indicating that the roasting reaction was still ongoing in the interior of the pile. This was impressively proven when the central inner parts of the roasting pile came to light. In some areas glowing charcoal was still present and the roasting reaction strengthened again in contact with oxygen. Unfortunately due to exterior constraints, we were forced to stop the roasting experiment. In order to stop the roasting reaction, as well as to cool down the ore and separate it from the remaining charcoal, the roasted ore was quenched in water-filled troughs.

All in all, the ore lost ~ 15 % of its initial weight. According to the appearance of the roasted ore pieces, the roasting reaction was successful in partially removing the sulfur from the ore: An intensively red surface had replaced the shiny yellow of the chalcopyrite ore. When broken open, the pieces revealed a sequence of a more than 1 mm thick layer of red colouration on the surface, purple-blue areas underneath it and unreacted chalcopyrite in the core (Figure 2, d). Near the thermocouple, the ore pieces were sintered and partially molten. As pure chalcopyrite has a melting point of ca. 950 °C, it is prob-

able that the temperatures reached in some parts of the roasting bed were higher than what was recorded by the single centrally-placed thermocouple. In preparation for smelting, the roasted ore was crushed to pieces between 5 and 10 mm in size.

### Smelting of the roasted ore in the shaft furnace

Like in the archaeological record from Bronze Age eastern Alpine smelting sites, the shaft furnaces were dug into the slope. The size and the concept of the furnaces are in accordance with the archaeological record (see above). The finished shaft furnace had a base of 40 x 45 cm<sup>2</sup> and a height of ~ 100 cm (Figure 3, a). To ensure a safe working environment, an area was cleared around the sides and back of the furnaces, which was level with the uppermost stones of the furnace shaft and covered with a layer of gravel as drainage (Figure 3, a). The furnace walls were constructed with firebricks using the above mentioned clay mixture as binder and to cover the inside surfaces. To record the temperature in the furnace, three cordierite tubes for the thermocouples were built into the centre of a side wall (Figure 3) with the lowermost (T1) at ~ 10 cm above the bottom of the furnace and the top one (T3) at ~ 40 cm. The bottom of the furnace was lined with several centimetres of clay to make a concave, slightly oblong bowl-like depression. The furnace walls were entirely lined with ~ 1 cm of clay. Before the furnace was used, an additional few millimetres of clay was applied.

The front wall only abutted the side walls so that it could be torn down and rebuilt after each smelt. In the lower part of the front wall, a ~ 25 cm wide and 20 cm high opening was left in which to place the two tuyères and a thermocouple (T4). These were kept in position with clay (Figure 3, c). The front wall was also built of the same firebricks and clay lining as the rest of the furnace, with the lower opening being spanned by a single larger firebrick. The base of the furnace mouth was roughly 10 cm above the lowest part of the furnace floor. The outlets of the tuyères were placed ~ 4 cm behind the inner limit of the furnace front wall at a slightly downward angle.

A total of 20 kg of roasted ore were smelted in each experiment. The furnace was fuelled with small split logs of coniferous wood no more than 10 cm in diameter, which were predominantly arranged parallel to the air flow in the furnace to allow the air to reach the back of the furnace. Preheating of the furnace without bellows took several hours to prevent the clay lining from cracking, and to allow a bed of coals to accumulate in the bottom of the furnace. As soon as 900 °C were recorded by the thermocouple placed between the tuyères (T4), the



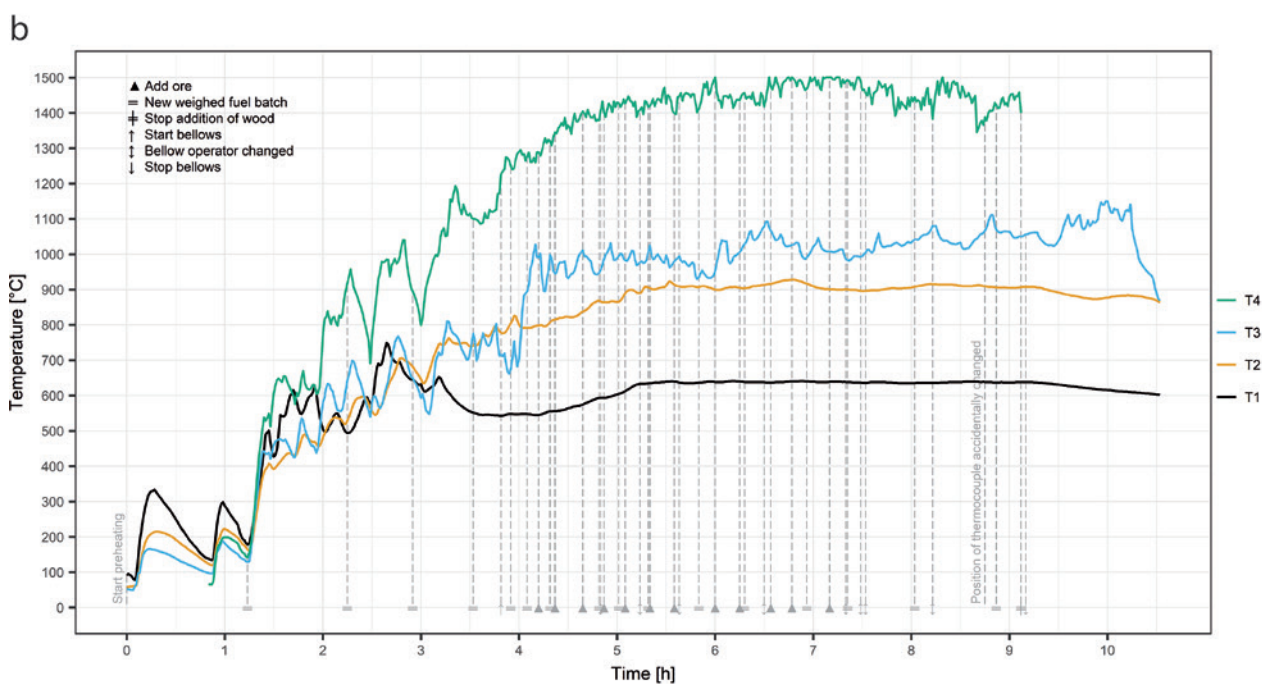
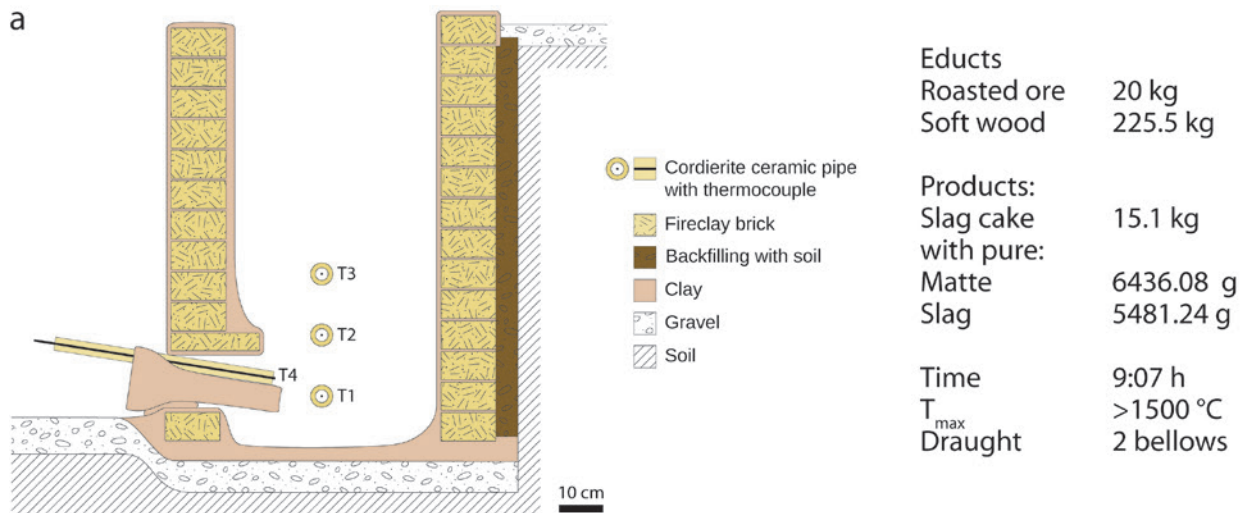


Figure 3. Smelting of the roasted ore, a) sketch of furnace; b) temperature curve; c) front view of the furnace with bellows and tuyères; d) furnace conglomerate (modified after Rose, Hanning and Klein, 2019).



bellows were attached and operated until a temperature of 1200 °C was reached. At this time, the more or less constant temperature of the two lowermost thermocouples in the furnace wall indicated they were entirely covered by ash and charcoal (Figure 3, b). During preheating, a bed of coals built up in the bottom of the furnace, on which the ore was able to rest and slowly move downwards through the furnace, giving it enough time to react.

Now the furnace was filled with wood and the first two charges (1 charge ~ 785 g) of ore were placed on top of the wood. This was repeated every 10 to 15 min. The furnace charge and fuel was periodically stoked from above with a wet wooden pole. Yellow smoke and the characteristic smell of sulphur indicated the beginning reaction of the ore. Once the ore reached the lower part of the furnace, temperatures above 1500 °C were periodically recorded by the thermocouple situated between the tuyères. After ~ 3 hours the entire ore charge was placed in the furnace. The addition of wood and the operation of the bellows continued for two more hours to give the last ore batch enough time to sink down and react. As the last step of the smelting procedure, the furnace was entirely filled with wood and allowed to burn down overnight. The tuyères and their thermocouple were removed before the furnace cooled down to keep the slag from solidifying on them.

The next day the front wall and the remaining charcoal were removed. However, the smelting products which accumulated at the bottom of the furnace were still so hot, that they had to cool down for another day until it was possible to remove them. The furnace conglomerate (i.e. the mass left in the bottom of the furnace after smelting the roasted ore, which consisted of an upper layer of slag with entrapped pieces of charcoal and unreacted ore and a lower layer of copper-iron-sulphides – the so-called matte) was in the middle of the bowl-shaped bottom of the furnace and had little contact with the furnace walls. There was also a layer of charcoal and ash separating it from the bottom of the furnace, making it easily detachable and leaving only minor damage to the clay lining. Slagged furnace wall was only observable around the furnace mouth.

Between 170 to 250 kg of wood was used in each experiment. Each furnace conglomerate weighed around 15 kg; additionally ~ 1 kg of unmelted ore was recovered from the charcoal. The slag and the matte were well separated from each other in the furnace conglomerate with the matte at the bottom, and a layer of slag attached at the top (Figure 3, d). The border between matte and slag was at the height of the tuyères' tips. However, a large quantity of charcoal was left in the matte, thus no solid block of matte was achieved. Only in the last experiment, S4,

larger pieces of matte were created. In this experiment denser, knotty wood was used for preheating. Unfortunately, the alumina protection tube of the thermocouple between the tuyères (T4) broke and the thermocouple was irreparably damaged by the slag. The other thermocouples indicated temperatures ~ 100 °C lower than in the previous experiments (see below). After the furnace conglomerate was thoroughly documented, it was crushed and the matte separated from the slag. Unmelted pieces of quartz from the gangue associated with the chalcopyrite ore were present in large quantities in the slag after all experiments while the ore minerals were fully liquefied.

## Roasting of the matte

Because archaeological evidences for the processing of the matte are exemplarily rare from the eastern Alpine regions, this step and the following ones are inspired by the traditional copper smelting process in Nepal (Anfinset, 2011; Goldenberg, et al., 2011). The matte from the previous step was ground to powder (< 1 mm). Also some slag pieces were ground and added to allow the iron in the matte to react with the free silica from the quartz-rich slag (additional silica and flux sources for the formation of the slag could also come from the fuel ash and clay furnace lining of the smelting pit, cf. Crew, 2000). The ground material was mixed with manure and shaped to ellipsoidal pellets of ~ 10 cm length. If the manure was too dry to form stable pellets, a bit of water was carefully added.

The wooden pile for roasting the manure pellets was built on the same roasting bed used for the ore. During roasting, the pellets become extremely brittle and tend to crumble easily. The fuel was stacked in a way that facilitated a complete oxidation of the pellets, as well as a vertical or at least inward-directed sagging of the burning wood to prevent as many pellets as possible from rolling off the pile and fracturing. To reach this aim, a trough-like construction with a base of 1 x 1.5 m<sup>2</sup> was built with coniferous wood: A thermocouple was placed in the centre of the pile and a layer of large logs was built as the base. For the next layer, a ring of large logs was placed at the rim of the pile and smaller logs were arranged to make a trough-like depression in the middle (Figure 4, a). A layer of bark and other small waste wood was placed on top of the logs and the pellets carefully placed on these (Figure 4, c). Straw was put into gaps between the large logs and set alight on several spots around the pile to set the whole pile on fire at the same time.

The roasting pile was left to burn down by itself without adding more fuel. Once in a while the characteristic

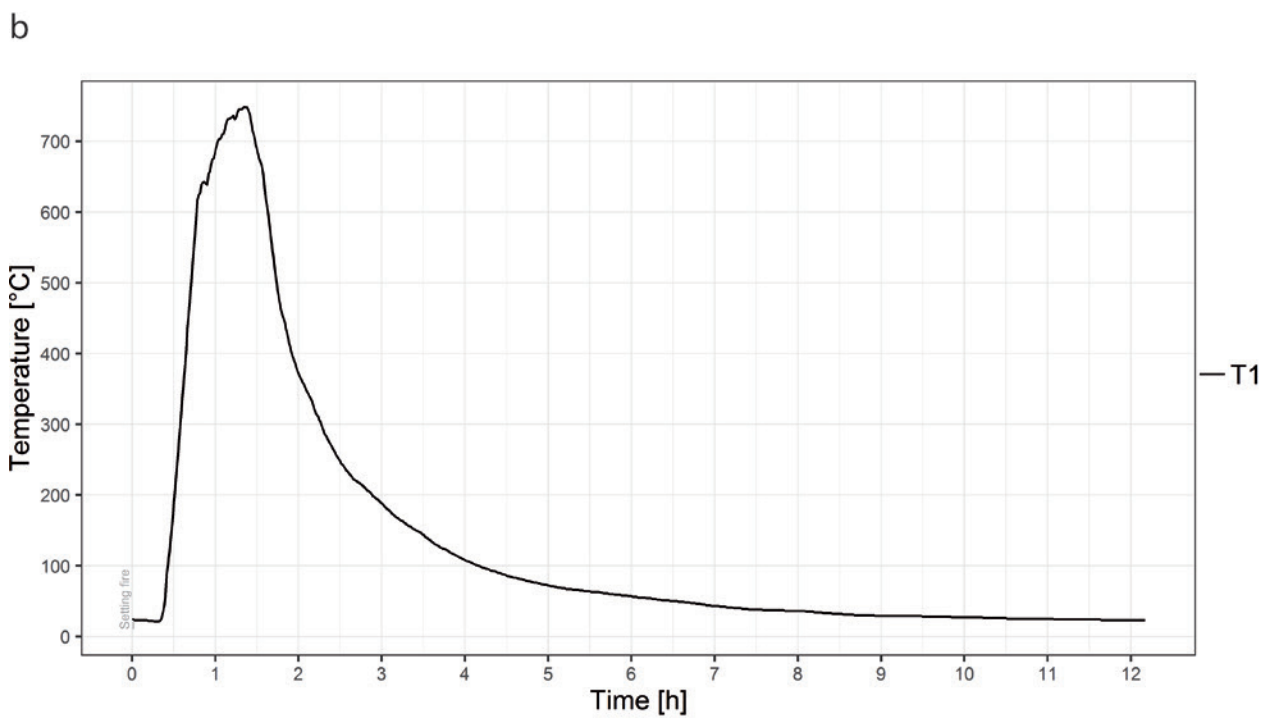
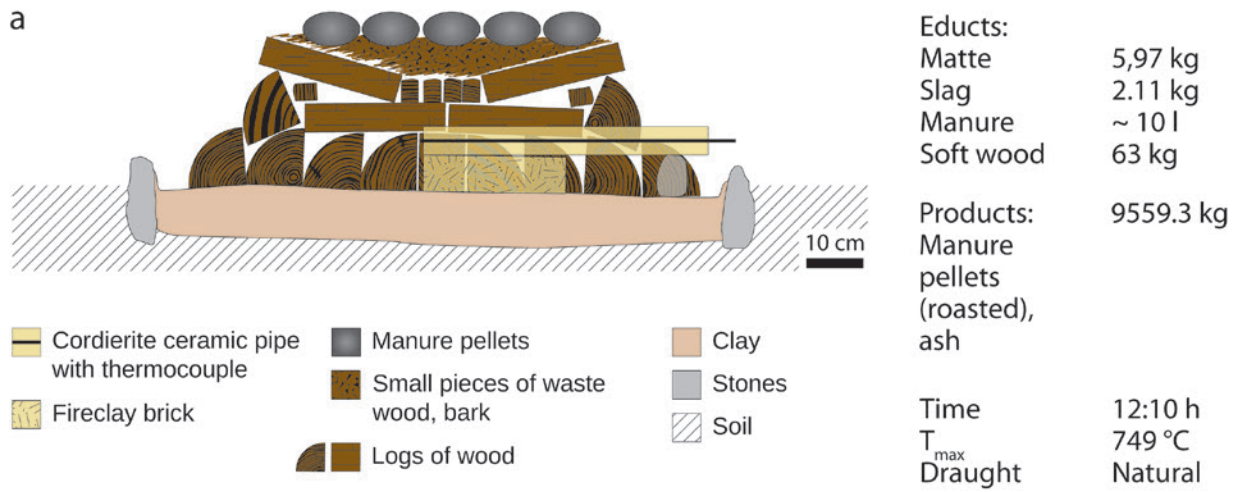


Figure 4. Roasting of the manure pellets, a) sketch of the roasting pile; b) temperature curve; c) roasting pile before fire is set; d) burned down roasting pile (modified after Rose, Hanning and Klein, 2019).

smell of sulphur was observed but it was considerably weaker than during the roasting of the ore. Maximum recorded temperatures reached in each experiment ranged between 750 and 981 °C (Figure 4, b). After the roasting experiment, about two thirds of the pellets remained in their original shape. The other ones were either broken into larger pieces or became powder (Figure 4, d), depending on the movement and mechanical stress when the pile burned down. Due to the flat smooth surface of the roasting bed, it was possible to sort out the larger pieces of charcoal and some of the ash, so that the broken pieces and powdered remnants of the matte balls could be swept together and added to the subsequent smelt.

### Smelting of the roasted matte

Because little is known about this process from the archaeological record, examples were again taken from ethnographic accounts, in particular the Nepalese smelting process mentioned above. First a pit with 30 cm diameter and 30 cm deep was dug into the ground and lined with several centimetres of clay. Two slits were dug into the rim to hold the tuyères in place. It soon became obvious that the original pit was too deep and that the lower layers of charcoal were too cold to keep the matte molten. Hence in most experiments, a large, shallow thick-walled crucible in the diameter of the pit was inserted to reduce its depth and covered with a layer of stamped charcoal dust. Several experiments with different arrangements and kinds of tuyères (straight or angled) were carried out. In the following, the most successful experiment S4p1 is described. This experiment was carried out with the same type of linear tuyères that were used for the smelting of the ore in the shaft furnaces and carried out directly in the pit, i.e. without the crucible.

The pit for the furnace was lined with several centimetres of clay and had an inner diameter of around 30 cm. Initially around 30 cm deep, the pit was filled with stamped charcoal powder up to 18 cm below the tuyères' outlets. Additionally, 4 cm of small pieces of charcoal were placed on top of the charcoal powder (Figure 5, a). The tuyères were placed opposite of each other with their outlets ~ 5 cm away from the pit rim and with a downward inclination of ~ 40°.

After a small fire was ignited in the pit, a bed of glowing charcoal was built up until ~ 5 cm above the pit rim, enclosing the tips of the tuyères entirely, and kept at this height throughout the entire experiment. The first batch of roasted manure pellets was cautiously placed in the middle of the glowing charcoal but not above the openings of the tuyères. At significantly more than 1000 °C, they slowly started to melt down into the pit. The next

batch of pellets was placed every 10 to 15 min, with each batch weighing ~ 400 to 900 g (Figure 5, b). After around 3.5 hours, a small hollow was made in the glowing charcoal in which all the remaining powder from the roasting experiment (mixture of roasted pellet material, ash and charcoal) was placed as the last batch. It was immediately covered by glowing charcoal to prevent the material from being blown away by the blast from the bellows. In total, 12.3 kg of material were introduced into the pit hearth and a maximum temperature of 1200 °C was reached. To reach this high temperature, it was necessary to produce short and strong air blasts with high frequency instead of the much longer and relatively gentle air blasts with a much lower frequency which were used when operating the bellows with the shaft furnace.

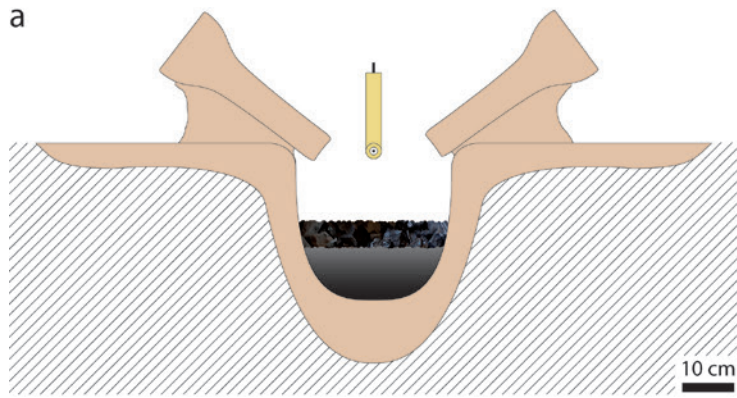
After roughly half of the material was melted, the charcoal was moved aside to check the state and amount of the melted material. It was already melted but still very viscous. About 25 min after the last batch was placed on the charcoal, everything was melted. The charcoal was removed again and this time it could be seen that the pit was filled with a liquid melt up to a few centimetres below the opening of the tuyères. The tuyères were removed and the melt was quenched by stroking it with a big brush made from a bundle of water soaked grass. Care was taken that the melt did not freeze on the furnace wall. Subsequently the thin plate of quenched melt was removed with a wet wooden stick and a shovel. This step was repeated eight times until the colour of the melt became brighter, signifying that the upper layer of slag had been removed and the lower layers of molten copper matte were becoming visible. The latter was quenched completely until it was solidified enough to take it out of the pit to cool down completely (Figure 5, c). Nearly no visible traces of slag and matte remained on the walls of the pits.


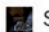



At the bottom of the matte, an aggregate of metallic copper weighing nearly 46 g and larger amounts of spongy copper were observed, but the spongy copper was too intimately intergrown with the matte in order to separate these two components. In total, 4.5 kg of slag and 3.6 kg of matte were produced. A closer examination of the thin slag plates revealed they were less than 5 mm thick and nearly entirely glassy (Figure 5, d).

### Smelting of the matte in graphite crucibles

Because not all the matte smelting experiments were as successful as the one described above, and the amount of matte became steadily smaller with each successive smelt due to loss of material during roasting (loss of sulphur) and smelting in the pit (slag phases and other sources of





 Cordierite ceramic pipe with thermocouple  
  Small charcoal pieces  
  Clay  
 Charcoal dust  
  Soil

Educts:  
 Manure pellets 12345.5 kg  
 Charcoal (roasted) 43.4 kg  
 Products:  
 Copper 45.92 g  
 Matte 3654.73 g  
 Slag 4626.41 g  
 Time 6:23 h  
 $T_{max}$  1200 °C  
 Draught 2 bellows

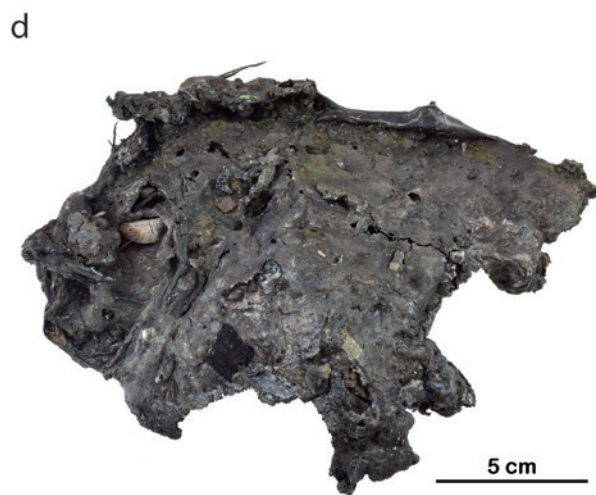
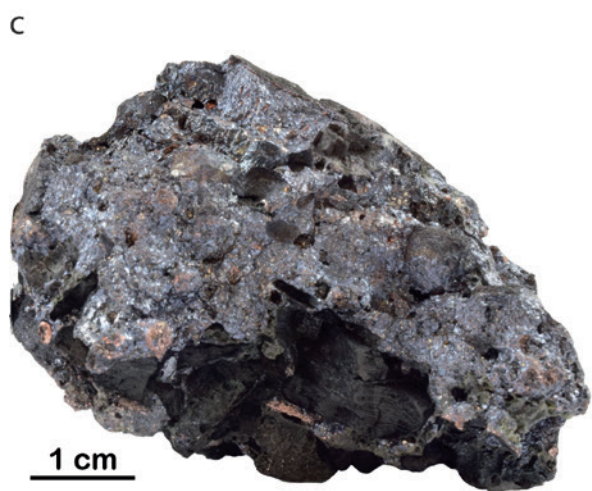
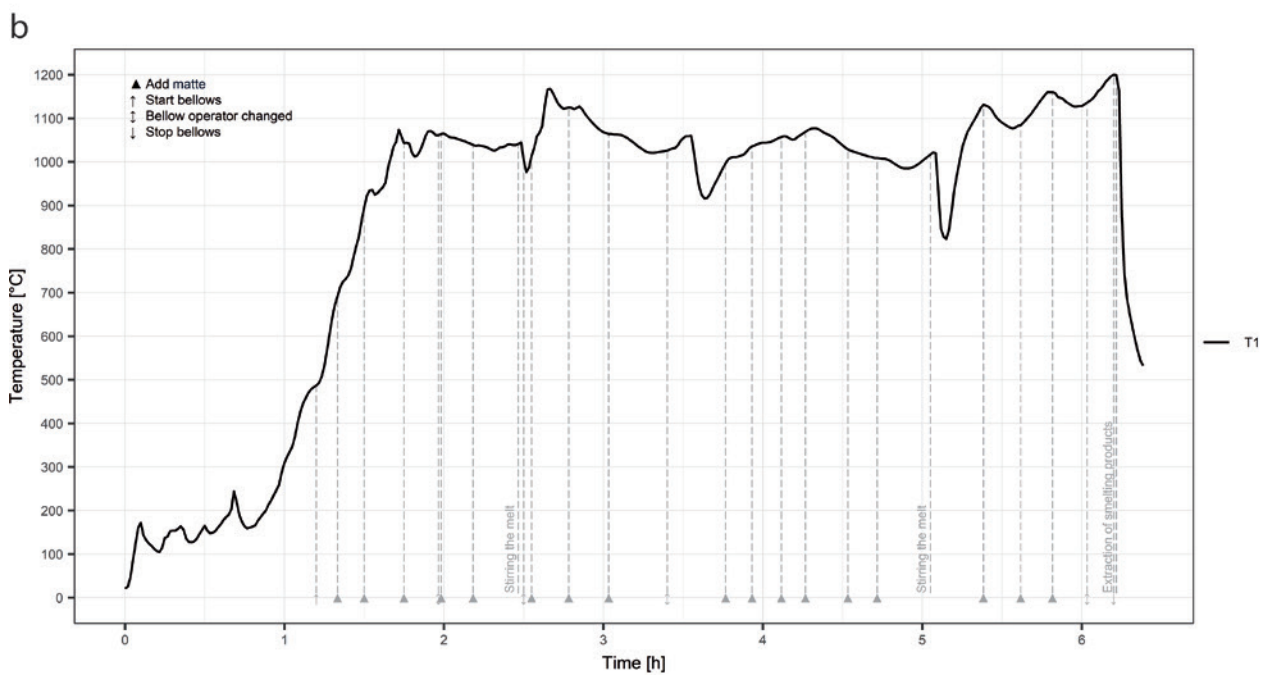


Figure 5. Smelting of the roasted manure pellets, a) sketch of the fire pit; b) temperature curve; c) matte smelted from the manure pellets; d) plate-like slag (modified after Rose, Hanning and Klein, 2019).

loss), we decided to refine the matte from some of the experimental series in smaller graphite crucibles. Due to time constraints, this was done on a charcoal bed with an artificial draft from below (electric bellows) in a smithing hearth at LEA. Artificial draft was provided by an electric fan from below. The temperature in the interior of the closed crucibles was not recorded to prevent the melt from freezing in contact with cold air. However the temperature of the charcoal bed surrounding the crucible was measured using an infrared pyrometer (Votcraft IR 2201-50D, -50 to 2200 °C, accuracy  $\pm 1.5\%$ ). The bottom of the crucible was filled with 60 g of charcoal dust to protect it from the melt and a layer of 100 g of quartz sand to provide silica for the formation of the slag. The matte was crushed and placed on top of the layer of sand.

After the material was mostly melted, the crucible was covered with a lid. After about 40 minutes, the matte was completely melted and the crucible was taken from the fire. Its content was then poured into an impression in a bed of quartz sand. In some cases, metallic copper settled onto the bottom of the impression, followed by a layer of matte and then slag on top. However, the graphite crucible proved to be too tightly covered by the lid and did not allow enough oxidization of the matte to further desulfurize the melt.

### Roasting and smelting of the matte in clay crucibles

Another approach was the roasting of the remaining matte and subsequent smelting in open, shallow clay



Figure 6. Smelting of the enriched matte, a) sketch of the experimental set-up; b) photograph of the fire pit (modified after Rose, Hanning and Klein, 2019).



crucibles. To achieve a larger surface for the roasting process, the matte was placed in a shallow oval crucible with a base of  $\sim 21 \times 12 \text{ cm}^2$  and a height of  $\sim 3 \text{ cm}$ , which was made from the same clay mixture used throughout the experiments. To prevent the bottom of the crucible from reacting with the matte, it was covered with a thin layer of sand and on top of that ground charcoal. The coarsely ground matte was placed in the crucible and roasted in an electric kiln to  $800 \text{ }^\circ\text{C}$  for 8 hours.

After it was cooled down completely, the crucible with the roasted matte was placed in a shallow pit furnace with a diameter and a depth of  $\sim 35 \text{ cm}$  and  $\sim 13 \text{ cm}$ , respectively. A single curved tuyère connected to an electric fan was placed with the outlet  $\sim 10 \text{ cm}$  from the rim and  $\sim 20 \text{ cm}$  above the bottom of the pit (Figure 6, a). The crucible was covered by thin pieces of coniferous wood and it was constantly checked that glowing charcoal or burning wood was between the tuyère and the crucible (Figure 6, b). Otherwise the cold air coming from the tuyère would have hit the surface of the crucible and have frozen the melt. The air blast coming from the tuyères was kept low and wood slowly but steadily added to the fire in order to slowly heat up the matte in hopes to further desulphurize it. About 2 hours later the matte was completely molten and the crucible taken out of the pit. The melt consisted of a top layer of slag with matte underneath and metallic copper at the bottom of the crucible. All in all,  $\sim 40 \text{ g}$  of metallic copper was produced in this experiment out of  $\sim 200 \text{ g}$  matte.

## Sampling

Experimental series S2 and S4 were chosen for sampling. S4 is regarded to be the most successful experiment series, in particular the experiments S4f1 and S4p1. The series S2 comprises the most remeltings which might be favourable to trace copper isotope fractionations. All materials were sampled on-site either before or after grinding of the smelting products for the next experiment. The naming scheme of the experiments as well as detailed information for each experiment is given in Rose, Klein and Hanning (2020).

## Methods

Analyses were carried out at the German Mining Museum Bochum (DBM) and are described in detail by Rose, Klein and Hanning (2020). With the exception of the pure metal samples, all samples were crushed in an agate

mortar and dried. XRD analyses were carried out with a PANalytical X'Pert Pro, using a Cu anode operated at  $45 \text{ kV}$  and  $40 \text{ mA}$ . The diffraction patterns were recorded between  $5^\circ$  and  $70^\circ 2\theta$ . GSAS II (Toby and Dreele, 2013) was used for Rietveld refinement of the obtained diffraction patterns. Crystal structures for comparison were taken from the American Mineralogist Crystal Structure Database (Downs and Hall-Wallace, 2003) and the Crystallography Open Database (Gražulis, et al., 2009; 2012). Crystal structures of some of the identified phases were not listed in the databases, thus not all samples allowed a semi-quantitative estimate of their phase composition. This is probably due to the fact that the Cu-Fe-S system has an extensive range of solid solutions and the synthetically produced phases from the smelting experiments do not always have an equivalent in the databases at hand. This circumstance restricted the interpretation of the data from these measurements to a qualitative level. Although the smelting products are anthropological materials and thus by definition not minerals (Nickel, 1995), the mineral names of the equivalent phases will be used here to ease readability.

Sample digestion for chemical analysis was carried out with a lab microwave (non-metallic materials) or on a hotplate (metals) using matrix-fitted acid mixtures (Rose, Klein and Hanning, 2020). The samples were diluted with water and  $5 \%$   $\text{HNO}_3$ , and measured with an ICP-SFMS Thermo Scientific Element XR. External calibration was used for quantification.

## Results

### X-Ray diffraction

Results of the Rietveld refined diffraction patterns are given in Table 1. When all diffraction peaks in a pattern were matched with a crystal structure, the concentration in wt. % is reported. If not, only the identified phases present in the sample are indicated. The limit of quantification in Rietveld refinement is usually around  $1 \text{ wt. } \%$  with a high relative error (León-Reina, et al., 2016). Hence all phases with a concentration less than  $2 \text{ wt. } \%$

Table 1 right. Phase composition identified from XRD patterns. "X" marks the presence of phases when quantitative refinement failed due to unknown phases or phases with unknown crystal structure (given in the last column). The lower wR % (parameter for the goodness of fit based on the sum of the residuals), the better is the fit between the calculated pattern and the measured one. Patterns for each sample are given in Rose, Klein and Hanning (2020).





are reported as < 2 wt. % or < 1 wt. %. The diffraction patterns of each sample and its refined pattern is given in Rose, Klein and Hanning (2020).

The ore consists of chalcopyrite ( $\text{CuFeS}_2$ ) and pyrite ( $\text{FeS}_2$ ) with accessory tetrahedrite ( $\text{Cu}_{10}(\text{Fe,Zn})_2\text{Sb}_4\text{S}_{13}$ ). The gangue comprises of quartz ( $\text{SiO}_2$ ), minor amounts of carbonates, and phlogopite ( $\text{KMg}_3(\text{Si}_3\text{Al})\text{O}_{10}(\text{OH})_2$ ) from the host rock. The bulk of the roasted ore consists predominantly of chalcopyrite, quartz, and haematite ( $\text{Fe}_2\text{O}_3$ ). Bornite ( $\text{Cu}_5\text{FeS}_4$ ) and magnetite ( $\text{Fe}_3\text{O}_4$ ) are major phases in the predominantly oxidised parts of the roasted ore. The reduced/unreacted part of the roasted ore shows a similar phase composition with a wider variety of Cu-Fe-S phases.

In the experimental series S2 only the matte from the first pit furnace experiment S2p1a yielded a refinement with quantitative data. In all experiments, bornite is a major phase. In experiment S2f1, troilite ( $\text{FeS}$ ) is also present. After the first matte roasting, all mattes of the S2 series also contain either chalcocite ( $\text{Cu}_2\text{S}$ ) or covellite ( $\text{CuS}$ ). Metallic copper was observed in all experiments and in experiment S2p1a a metallic iron phase, too. The quartz in S2p3c4 indicates remnants of the quartz sand layer in the clay crucible.

In contrast to series S2, the S4 series' mattes contain troilite beside the ubiquitous bornite until the second matte roasting. The matte of S4f1 also contains cubanite ( $\text{CuFe}_2\text{S}_3$ ). Experiment S4p2 is the only experiment after the first matte roasting with a chalcocite-free matte. No covellite was observed throughout the S4 series experiments. Metallic copper is present in all mattes. Metallic iron or a Fe-Ni alloy was produced in the experiments S4p2 and S4p2c1.

The slag from all experiments contains pyroxenes (hedenbergite,  $\text{CaFeSi}_2\text{O}_6$  or ferrosilite,  $(\text{Fe,Mg})_2\text{Si}_2\text{O}_6$ ). With the exception from the shaft furnace experiments, fayalite ( $\text{Fe}_2\text{SiO}_4$ ) is also present throughout. Troilite appears only in the slags from the shaft furnace experiments. In series S2 magnetite ( $\text{Fe}_3\text{O}_4$ ) is present in all experiments, while it is missing in S4 experiments except for S4p2c3. Only the slags from series S2 contain metallic copper. After the second roasting, the slag in both experimental series is dominated by magnetite and fayalite. Pyroxenes (and fayalite) tend to be the major phases in all other experiments.

The first matte roasting (with manure pellets) yielded in both series besides bornite, mostly hematite and besite ( $\text{Ca}_{1.18}\text{Fe}_{0.9}\text{Mn}_{0.92}(\text{PO}_4)_2$ ). Cristobalite ( $\text{SiO}_2$ ) and

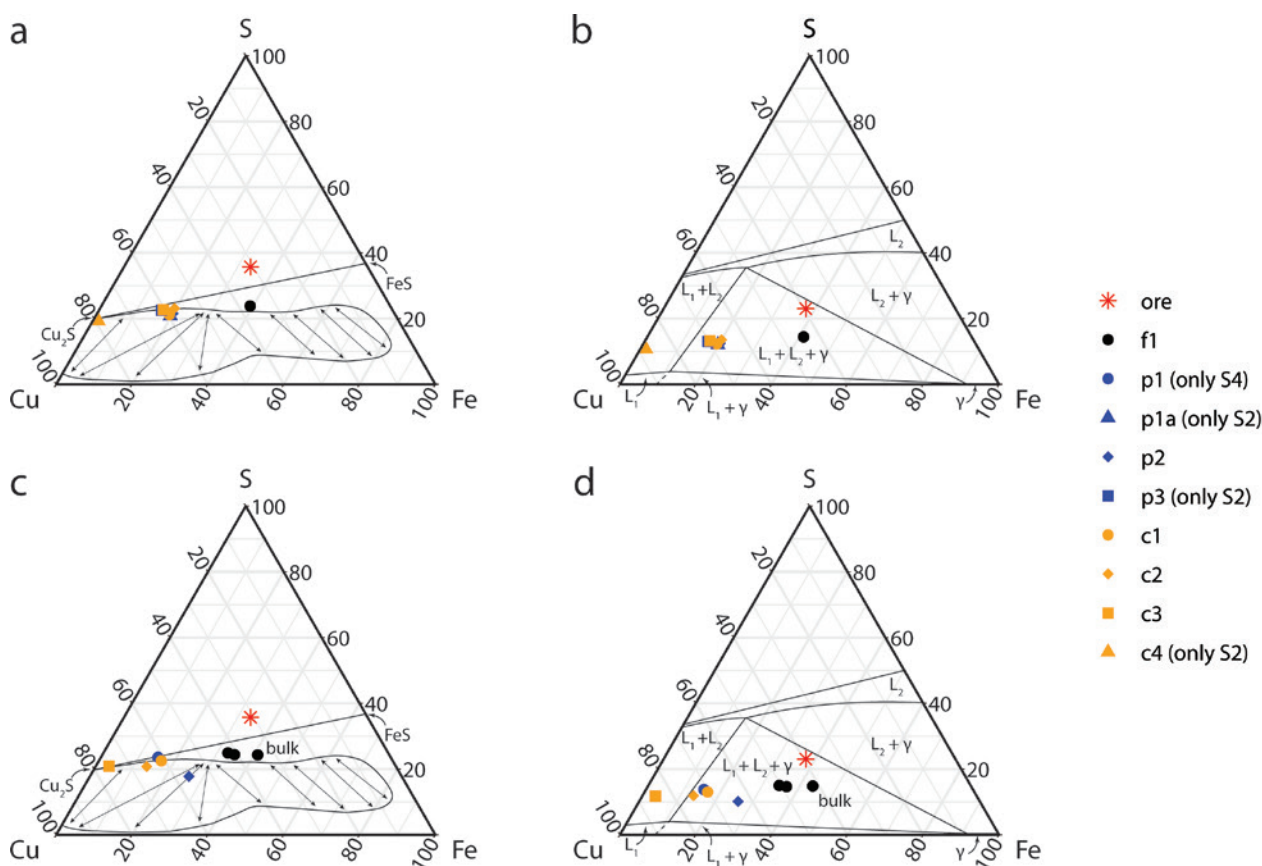


Figure 7. Cu-Fe-S diagrams of the matte from different experiments for the experimental series S2 (a, b) and S4 (c, d); a, c in wt. % with the miscibility gap given in Hentze (1929), b, d in at. % with phase boundaries taken from Chang, Lee and Neumann (1976), all at 1200 °C and 1 atm.

Table 2. Cu, Fe, and S concentrations in wt. % of the chalcopyrite ore and of the matte obtained in the different experiments. Concentrations of all measured elements are given in Rose, Klein and Hanning (2020).

| Sample        | Material | Experimental set-up | Cu   | Fe   | S    | Total |
|---------------|----------|---------------------|------|------|------|-------|
| Cpy6          | Ore      |                     | 21.0 | 22.7 | 24.3 | 101.6 |
| S2f1-m        | Matte    | Shaft furnace       | 28.3 | 30.0 | 18.3 | 98.1  |
| S2p1a-m       | Matte    | Pit furnace         | 54.3 | 17.9 | 19.0 | 100.7 |
| S2p2-sm-m     | Matte    | Pit furnace         | 51.8 | 17.7 | 19.1 | 100.8 |
| S2p3-m        | Matte    | Pit furnace         | 59.0 | 16.0 | 21.8 | 98.2  |
| S2p3c1-m      | Matte    | Graphite crucible   | 56.1 | 18.1 | 20.0 | 97.4  |
| S2p3c2-m      | Matte    | Graphite crucible   | 55.4 | 19.0 | 22.4 | 98.7  |
| S2p3c3-m      | Matte    | Graphite crucible   | 58.2 | 16.3 | 21.9 | 98.6  |
| S2p3c4-m      | Matte    | Clay crucible       | 73.9 | 1.34 | 18.0 | 95.5  |
| S4f1-m (bulk) | Matte    | Shaft furnace       | 22.8 | 27.0 | 16.0 | 94.0  |
| S4f1-m2-1     | Matte    | Shaft furnace       | 40.1 | 31.2 | 23.7 | 96.9  |
| S4f1-m4       | Matte    | Shaft furnace       | 37.7 | 32.2 | 22.5 | 93.8  |
| S4p1-m-1      | Matte    | Pit furnace         | 57.5 | 14.1 | 22.1 | 95.8  |
| S4p2-m        | Matte    | Pit furnace         | 49.0 | 22.8 | 15.5 | 92.6  |
| S4p2c1-m      | Matte    | Graphite crucible   | 56.2 | 15.1 | 20.7 | 99.0  |
| S4p2c2-sm     | Matte    | Graphite crucible   | 63.0 | 12.9 | 19.9 | 97.7  |
| S4p2c3-sm     | Matte    | Clay crucible       | 65.7 | 3.07 | 18.1 | 89.1  |

fayalite are minor phases in both experiments. Magnetite, copper sulphides, pentlandite ((Fe,Ni)<sub>9</sub>S<sub>8</sub>), and traces of pyroxenes are observed only in S4r1. Samples of the second matte roasting (in a clay crucible) were acquired only from series S4 and consist beside bornite mostly of chalcocite and hedenbergite with smaller amounts of quartz and kieserite (MgSO<sub>4</sub>·H<sub>2</sub>O).

## Chemical analyses

Only the main elements Cu, Fe, and S are reported (Table 2) because trace elements have no significant impact on the smelting process and a full discussion of the data set is beyond the scope of this contribution. They sum up close to 100 % for all samples except for the mattes from the shaft furnace experiments, S2f1-m and S4f1-m, where significant concentrations of SiO<sub>2</sub>, Al<sub>2</sub>O<sub>3</sub>, CaO, and MgO indicate the presence of slag.

Plotting all matte samples in the Cu-Fe-S system (Figure 7) shows a relatively uniform sulphur concentration in all mattes and a very similar composition of the respective experiments from both experimental series. The matte from the shaft furnace experiment (f1), from the pit furnace experiments (p1 to p3), and from the experiment in an open clay crucible (S2p3c4-m, S4p2c3-m)

are clearly separated from each other and show a trend towards a lower iron content. The experiments carried out in graphite crucibles (S2p3c1-m to S2p3c3-m, S4p2c1-m and S4p2c2-m) show a composition similar to the pit furnace experiments. All of them plot close to the sulphur-rich border of the miscibility gap of the Cu-Fe-S system (Figure 7). The only exception from this overall picture is S4p2-m, which shows a lower S and higher Fe content compared to the other pit furnace experiments and plots within the miscibility gap.

## Discussion

### Roasting of the ore

The mineralogical composition of the ore sample Cpy6 matches the mineralogy of ores from the Mitterberg (Bernhard, 1965). According to Bernhard (1965) pyrite in the Mitterberg ore can contain a significant amount of Ni. The Ni will enrich in the matte during smelting (Tylecote, Ghaznavi and Boydell, 1977), which might explain the occasional presence of millerite (NiS), pentlandite and of the Fe-Ni alloy.

The zonation visible in the roasted ore (Figure 2, d) – hematite on the surface followed by a dark layer rich



in spinels, a bluish layer of various Cu-Fe-S phases, and unreacted chalcopyrite in the core – is also in agreement with literature data (Burger, et al., 2011). The growth of numerous small crystals on the surface of the roasted ore pieces (Figure 8) in combination with the presence of sulphates in the diffraction patterns indicates the formation of secondary minerals. Admittedly, the success of the roasting experiment was unanticipated concerning the duration and intensity of the self-sustaining roasting reaction about 24 hours after the last fuel was added, even though the roasting reaction had to be stopped due to exterior constraints. During quenching, the water quickly became green-bluish, indicating significant dissolution of copper. The pH test strip indicated a pH ~ 1. Presumably the sulphur-containing gases or sulphur precipitated on the colder surface of the roasting pile dissolved in the water as sulphuric acid. To minimise copper loss, the roasted ore was taken out of the water as soon as possible and dried in the sun. Growth of secondary phases might be either initiated by drying or during the storage of the roasted ore for several months until the beginning of the smelting experiments. During this time, the fine material consolidated into a pale grey-greenish friable crust, and on the uppermost pieces, the abovementioned secondary minerals grew as fine crystals on their surface. The magnesium and calcium necessary for the growth of kieserite and anhydrite ( $\text{CaSO}_4$ ), respectively, might be derived from the wood ash (Matthes, 2018, p.456) that dissolved during quenching.

The design of the roasting experiment was successful in keeping the self-sustaining roasting reaction ongoing. During the removal of the pile remains, it became obvious that the layer of ash and fine material on top of the pile not only kept in the heat but also inhibited the flow of oxygen into the middle of the roasting pile. This must have been happened very quickly, as some of the larger logs in the interior were not entirely charred. Thus, modifications towards a longer lasting flow of air into the centre of the pile might be preferable. However, due to time constraints and lack of more unroasted ore, it was not possible to carry out more than one roast.

## Smelting experiments

### Smelting of the roasted ore in the shaft furnace

The two smelting experiments in the shaft furnace were successful in separating the matte from the slag. The matte, due to its higher density, collected at the bottom of the furnace, covered by a layer of slag. However, the layer of matte was not compact but contained a high proportion of charcoal and did not separate easily from the overlying slag like in other experiments. This could be

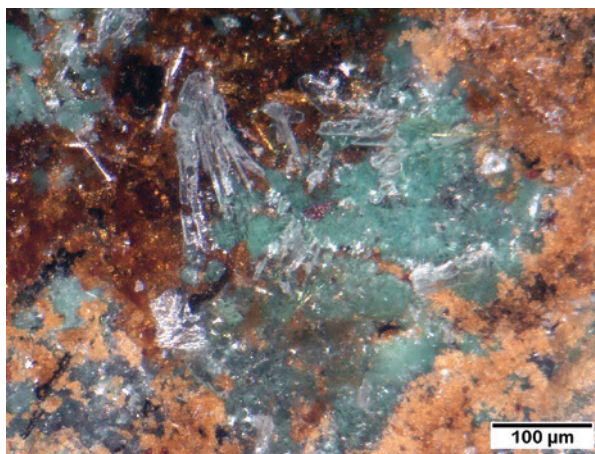


Figure 8. Secondary minerals (translucent needles and radiating green aggregates) on the surface of a roasted ore piece (photomicrography). Photo: Th. Rose.

partly due to the fact that (matte-rich) slag from previous experiments was not added as flux, in order to prevent mixing of materials from different experimental series (see Hanning and Pils, 2011).

In S4f1, at least some larger lumps of matte were formed. However, the slag was mostly massive with nearly no entrapped charcoal, but with some lenses of entrapped matte and occasionally small prills of metallic copper. This might indicate that the tuyères were not perfectly positioned. A lower position of the tuyères might enhance the removal of sulphur. However, based on experiences from previous experiments carried out by E. Hanning, if the tuyères were positioned too close to the furnace floor, they became blocked by slag most of the time, resulting in a premature end of the smelt. Probably a steeper downward angle would be a working compromise. A lower position or steeper downwards angle of the tuyères would also introduce more oxygen into the lower part of the furnace, which might enhance the removal of sulphur and the oxidation of iron in the matte, facilitating the subsequent steps of copper smelting. Alternatively, preheating of the shaft furnace could be carried out with larger logs to create larger voids in the remaining charcoal. For experiment S4f1 large logs of predominantly knotted wood were used, while in S2f1 the small logs were used, which were also used as fuel for the smelting phase. This might have resulted in some bigger cavities, providing enough space to allow the formation of the larger lumps of matte.

### Smelting of the matte in the pit furnace

Except for S2p1a and S4p1, the pit furnace experiments struggled to produce a liquid slag and melt. Only in experiment S4p1 a low viscous melt was achieved where thin plates of slag could be extracted. The effect of sul-

phur as an additional heat source was noticeable in all experiments, but only in experiment S4p1 did the recorded temperatures reach around 1200 °C (i.e. the melting point of fayalite) and thus lead to the low viscosity of the melt. At the same time, this experiment was the only one which produced larger amounts of copper and copper sponge.

The reason for this success was most likely a different way to operate the bellows. Inspired by traditional Nepalese copper smelting, short, strong air bursts were produced in a high frequency instead of the longer, gentle air bursts in previous experiments. Moreover, the bellow technique in this experiment was not the only difference to the previous experiments but also the steep angle of the tuyères, which directed the air flow directly onto the surface of the melt. Unfortunately the subsequent experiments using this arrangement (S4p2, S2p3) were not successful in producing a liquid slag.

Removing the slag from the furnace layer by layer by cooling the upper crust of slag with a water-soaked brush made of grass was very successful. The melt did not harden and bind itself to the clay-lined walls, and could be easily extracted from the pit. It is also noteworthy that the pit furnace lining did not show any damage and very little sign of metallurgical activity, besides being heated to high temperatures, after the end of the experiment. Hence, pits impacted by heat found in the archaeological record at smelting sites should definitely be taken into account as possible installations for smelting matte, even if they bear no visible traces of metallurgical activities.

### Crucible smelting

Except for S4p2c1 none of the experiments with graphite crucibles yielded metallic copper, most likely due to the closed, deep cylindrical form of the crucible. This did not allow enough contact with the air to further desulphurize the melt. Also the remaining iron could not oxidize and be removed from the melt in the form of slag. Without depletion of sulphur and iron from the melt, the matte composition remained stable and no metallic copper will precipitate. Furthermore, the molten matte, when poured from the crucible onto the sand bed, cooled too quickly to undergo any significant amount of oxidation. Additionally, it cannot be excluded that the copper yielded in S4p2c1 was already present within the matte e.g. as spongy copper from experiment S4p1.

In contrast to the graphite crucibles, the open, shallow form of the clay crucibles worked very well. The roasted matte was exposed to a constant supply of air, allowing a further oxidation of the iron and the sulphur. As a result, experiments in both experimental series were successful in producing larger amounts of metallic

copper on the bottom of the crucible, followed by a layer of residual matte and a layer of slag on top.

### Matte

The chemical composition of the matte obtained from the same experimental setup is very similar in the two experimental series (Figure 7). The strong shifts in the iron content after each roasting step, and the same chemical compositions of the matte from the pit furnace experiments and the graphite crucible experiments, except for S4p2, evidences the efficient depletion of iron by its oxidation during roasting and subsequent transfer into the slag during smelting.

Beside the chemical similarities in the matte of both experimental series, substantial differences do exist. They are particularly striking with respect to the copper yields and indicate more favourable conditions for the production of copper in the S4 series: In the shaft furnace, S4f1 produced 25.25 g of copper prills, while none were produced in S2f1. After the first matte roasting, both, S2p1a and S4p1 yielded metallic copper. However, the amount from S4p1 was four times higher (45.92 g + sponge copper vs. ~ 12.29 g from the S2 experimental series). Additionally, S4p2c1 was the only experiment in a graphite crucible that yielded metallic copper.

Because the same roasted ore was used and the general experimental setup of the shaft furnace experiment was the same, differences during this experiment must have occurred in the operation of the furnace. Due to the failure of T4 during the experiment S4f1 little can be said about the maximum temperature reached. The much steeper rise of the temperature at the tuyères in S4f1 might indicate an overall higher temperature in front of them. Additionally, the tip of the tuyères was ~ 4 cm deeper into the furnace, which successfully prevented them from clogging with molten furnace wall like in the previous experiments. At the same time, T2 and T3 indicate a consistently lower temperature and T3 also had less fluctuation. The temperatures of T1 and T2 in S4f1 are closer to the ones measured at T3, resulting in higher temperatures at T1 in the second half of the experiment compared to S2f1.

Based on the temperature distribution, a cooler but more homogeneously heated furnace was operated in S4f1. This might have resulted in a slower speed of the roasted ore moving down into the furnace and thus a prolonged time to roast before it became molten. This is supported by the circumstance that although the shaft furnace was operated longer in experiment S4f1 than S2f1, 1149.61 g of the ore remained unmelted compared

to 221.37 g, respectively. Further, the placement of the ore took more than an hour longer in experiment S4f1, giving the ore and the melt more time to react.

Such differences in the furnace conditions can be correlated with differences in the phase composition of the respective smelting products. While cubanite, troilite and copper were the only Cu-Fe-S phases in experiment S4f1, small amounts of valleriite ( $\text{Cu}_2\text{Fe}_4\text{S}_7$ ) and the low-temperature phase mooihoekite ( $\text{Cu}_9\text{Fe}_9\text{S}_{16}$ ) (Raghavan, 2004) are present in the smelting products of S2f1 together with bornite and troilite, indicating more heterogeneous conditions at least during cooling in the latter experiment. Further, the presence of cubanite as (main) Cu-Fe-S phase indicate a higher amount of oxidised iron in the matte of experiment S4f1 compared S2f1. In cubanite, one of the two Fe atoms is present as Fe(III) (Gibbs, et al., 2007; Goh, et al., 2010), giving ~ 16.7 at % of Fe(III) in it. Bornite contains only one Fe atom. Its oxidation state is unclear and can be most likely described best as + 2.5 (Goh, et al., 2006; Mikhlin, et al., 2005). However, even if the Fe in bornite would consist entirely of Fe(III), it would reach a proportion of only 10 at %. This indicates a higher amount of iron in the matte of S4f1, probably because the lower temperature in the furnace limited the availability of  $\text{SiO}_2$  to produce slag (matte to slag ratio in S2f1 1:1, in S4f1 1.55:1). At the same time, less copper can be structurally included in cubanite than in bornite. Consequently, copper will segregate as elemental copper, which was present as a smelting product only in the experiment S4f1.

The copper peaks in the diffraction data of both experiments indicate that some metallic copper remained within the matte. Due to the miscibility gap, the chemical composition of the final matte in both experiments cannot be that different and might be balanced by the amount of troilite and metallic copper in the matte.

Although not evidenced in the phase composition of the roasted material, the conditions of the first matte roasting in S4r1 might have supported a more efficient roasting process in the S4 series. The maximum temperature was more than 200 °C higher and the manure pellets were smaller, giving a higher reactive surface. Taken together, iron oxidation seems to be significantly enhanced in the S4 series from its beginning. This significantly facilitated the production of metallic copper in the subsequent experiments and laid the foundations for the successful smelting of the matte to copper in S4p1.

In contrast to this experiment, experiment S4p2 failed: although similar temperatures were reached, no copper was produced, although copper is present in the matte S4p2-m. Additionally, it is the only experiment that plots inside the miscibility gap (Figure 7). Based on

the appearance of the smelting products, it seems that in this experiment the distance between the hot area and the bottom of the pit was too great. The material was molten, but solidified at the bottom of the pit without having the time to segregate the copper. Additionally, the very high matte to slag ratio of 3.3:1 might indicate insufficient silica to react with the available iron in the furnace charge and thus prohibiting further depletion of the iron content of the matte. In the subsequent experiment S4p2c1, conditions were finally favourable for a liquid melt and the copper already present in the matte could segregate.

## Slag

Comparing the phases present in the slag with the oxygen fugacity and temperature ranges that they are stable in (Lindsley, 1967), can give information about the redox conditions in the furnaces/crucibles. The phase compositions of all experiments plot around the fayalite-magnetite-quartz equilibrium (Figure 9). In the shaft furnace experiments, slightly less reducing conditions are indicated by the absence of fayalite in the slag S2f1-s and the slag-matte mixture S4f1-fm. The formation of pyroxenes might have been additionally favoured by the

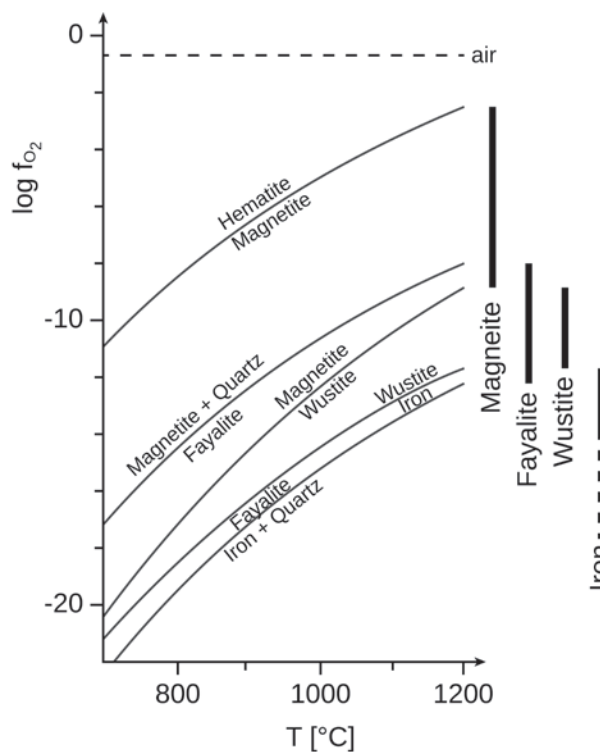


Figure 9. Oxygen fugacities ( $f_{\text{O}_2}$ , in atm) as a function of temperature at a pressure of 1 atm for the solid-solid-buffers relevant for slags. On the right, the stability ranges of the most important slag phases are shown at  $T = 1200$  °C (Lindsley, 1967).



large amounts of Ca derived from wood ash (~25 % CaO in coniferous wood, and 42 to 56 % CaO in beech wood (Matthes, 2018)).

## Conclusions

The smelting experiments with chalcopyrite ore based on archaeometallurgical evidence of the Bronze Age Eastern Alps and modern Nepal were successful in producing metallic copper.

Two out of the four experimental series (S2 and S4) were chosen for analysis. Both of these yielded metallic copper, slag and matte in collectable quantities. Especially the experiments in series S4 provided favourable conditions for the successful smelting of chalcopyrite ore to metallic copper and matte. Based on observations of the furnace performance, chemical data of the matte and the phase composition of the smelting products, the iron in the furnace charge was more extensively oxidised in the shaft furnace experiment with roasted ore S4f1 than in S2f1. Additionally, the significantly higher temperature in the subsequent roasting experiment might have enhanced this effect. Moreover, the pit furnace experiment with roasted matte S4p1 allowed us to extract several layers of platy slag similar to the ones found in the archaeological contexts of the Bronze Age Eastern Alps. In addition a relatively larger amount of sponge copper as well as ~ 45 g of massive metallic copper was also produced. A prolonged duration of the experiment might have been sufficient to continue extracting copper from the matte. After the experiment, the pit showed no clear visible traces of metallurgical activity. Hence, pit furnaces used for matte smelting might not be identifiable in the archaeological record by a visual assessment only and would require chemical analysis of the pit lining and contents to ascertain if metallurgical activity occurred in them.

Experiments in graphite crucibles did not yield any metallic copper, probably because most of the oxygen reacted with the fuel and/or the crucibles were too high to allow a sufficient influx of oxygen without forced draft from the top. Only with the second matte roasting and the subsequent smelting in open clay crucibles was copper produced in larger quantities in both experimental series.

Especially the chemical data of the matte clearly shows the significance of roasting for a successful smelting process. Substantial removal of iron in the form of slag was only achieved in the smelting experiments directly following the roasting experiments. In both experiment series, it seems that after the smelting of the

ore in the shaft furnace, two cycles of roasting the matte and subsequent smelting with a sufficient source of silica (most likely a combination of non-reacted silica from ground-up slag from a previous step, silica from the fuel ash or from the furnace lining) would have been sufficient to remove most of the iron from the matte in the form of slag.

Although valuable information about e. g. the way to operate the bellows for matte smelting was obtained, we were not able to reproduce the conditions of the most successful matte smelting experiment S4p1. We also did not manage to produce compact matte cakes in the shaft furnace. Solving these problems and getting closer to a substantial recovery of metallic copper requires more experiments. To facilitate such future experiments, the parameters of all experiment types have been described in detail and potential improvements of the experimental setups were given. Additionally, the key data for every single experiment is given in Rose, Klein and Hanning (2020). At the same time, the experiments and their detailed documentation serve as a material basis for future research on the behaviour of different elements and isotopes in the chalcopyrite smelting process.

The results of the behavior of the copper isotope fractionation during the experiments have been discussed in detail in a separate article (Klein and Rose, 2020). In general it can be said that although the fractionation of Cu isotopes between the ore and produced Cu metal is not particularly evident from the experiments, there was, however, measurable fractionation in particular for copper prills trapped in the slag whenever heterogeneous temperature zones cause different cooling rates. Further, foreign Cu sources from the flux and furnace lining, and especially their natural Cu content influenced the copper isotope signature of the slag components. Additionally, certain decisions made during the smelting process, for example quenching the roasted ore in water, also influenced the copper isotope ratios (see Klein and Rose, 2020). Copper isotope fractionation has to be considered for copper prills above all in highly viscous slags. Such slags were potentially re-melted to increase the metal yield. Hence, the copper gained in a subsequent melting step is potentially different in isotope composition when compared to ore and solid copper from the first smelting.

## Acknowledgements

This work received funding from the Deutsche Forschungsgemeinschaft (KL 1259/10-1). We would like to thank the head of the RGZM Laboratory for Experimental Archaeology, Michael Herdick, for the use of the

Laboratory and Facilities for the experiments. He did a great job in managing the administrative requisites at the RGZM and getting the necessary permissions. The experiments would have been impossible without the substantial efforts of Anna Axtmann, Sajuri de Zilva, Joseph Engelmann, and the 14 student volunteers. The authors are grateful to Jan Sessing for the XRD analyses, and Michael Bode and Regina Kutz (all DBM) for the chemical analyses. The helpful comments of the anonymous reviewers are gratefully acknowledged.

## Notes

- 1 It was decided to use the Bronze Age Alpine copper smelting process for the reconstruction due to the experience already gained with this technology from experiments run by E. Hanning as part of her PhD thesis (Hanning, in prep).
- 2 The ore was collected by E. Hanning as part of her PhD thesis work and was made available for the experiments.

## References

- Agricola, G., 1556 [2006]. *De Re Metallica Libri XII: Zwölf Bücher vom Berg- und Hüttenwesen*. Wiesbaden: Marix.
- Anfinset, N., 2011. *Social and technological aspects of mining, smelting and casting copper: An ethnoarchaeological study from Nepal*. Veröffentlichungen aus dem Deutschen Bergbau-Museum Bochum, 181. Bochum: Deutsches Bergbau-Museum.
- Asael, D., Matthews, A., Bar-Matthews, M. and Halicz, L., 2007. Copper isotope fractionation in sedimentary copper mineralization (Timna Valley, Israel). *Chemical Geology*, 243(3-4), pp.238-254. <http://dx.doi.org/10.1016/j.chemgeo.2007.06.007>.
- Asael, D., Matthews, A., Bar-Matthews, M., Harlavan, Y. and Segal, I., 2012. Tracking redox controls and sources of sedimentary mineralization using copper and lead isotopes. *Chemical Geology*, 310-311, pp.23-35. <http://dx.doi.org/10.1016/j.chemgeo.2012.03.021>.
- Asael, D., Matthews, A., Oszczypalski, S., Bar-Matthews, M. and Halicz, L., 2009. Fluid speciation controls of low temperature copper isotope fractionation applied to the Kupferschiefer and Timna ore deposits. *Chemical Geology*, 262, pp.147-158. <http://dx.doi.org/10.1016/j.chemgeo.2009.01.015>.
- Bachmann, H.G., 1993. Vom Erz zum Metall (Kupfer, Silber, Eisen) - Die chemischen Prozesse im Schaubild. In: H. Steuer and U. Zimmermann, eds. 1993. *Alter Bergbau in Deutschland*. Stuttgart: Theiss. pp.35-40.
- Bernhard, J., 1965. Die Mitterberger Kupferkieslagerstätte: Erzführung und Tektonik. *Jahrbuch der Geologischen Bundesanstalt*, 109, pp.3-90.
- Bower, N.W., Hendin, D.B., Lundstrom, C.C., Epstein, M.S., Keller, A.T., Wagner, A.R. and White, Z.R., 2013. "Biblical" bronze coins: New insights into their timing and attribution using copper and lead isotopes. *Archaeological and Anthropological Sciences*, 5(4), pp.287-298. <http://dx.doi.org/10.1007/s12520-012-0113-4>.
- Burger, E., Bourgarit, D., Frotté, V. and Pilon, F., 2011. Kinetics of iron-copper sulphides oxidation in relation to protohistoric copper smelting. *Journal of Thermal Analysis and Calorimetry*, 103(1), pp.249-256. <http://dx.doi.org/10.1007/s10973-010-0926-2>.
- Chang, Y.A., Lee, Y.E. and Neumann, J.P., 1976. Phase Relationships and Thermodynamics of the Ternary Cu-Fe-S System. In: J.C. Yannopoulos and J.C. Agarwal, eds. 1976. *Extractive metallurgy of copper: Vol. 1, Pyrometallurgy and electrolytic refining*. New York: AIME. pp.21-48.
- Crew, P., 2000. The influence of clay and charcoal ash on bloomery slags. In: C. Cucini Tizzoni and M. Tizzoni, eds. 2000. *Il ferro nelle Alpi = Iron in the Alps: Giacimenti, miniere e metallurgia dall'antichità al XVI secolo: atti del convegno, Bienno (BS), Italy, 2-4 ottobre 1998*. Bienno: Comune di Bienno. pp.38-48.
- Czedik-Eisenberg, F., 1958. Beiträge zur Metallurgie des Kupfers in der Urzeit. *Archaeologia Austriaca*, Beiheft 3, pp.1-18.
- Downs, R.T. and Hall-Wallace, M., 2003. The American Mineralogist Crystal Structure Database. *American Mineralogist*, 88, pp.247-250.
- Fasnacht, W., 2010. 20 Jahre Experimente in der Bronzetechnologie: eine Standortbestimmung. *Experimentelle Archäologie in Europa*, 9, pp.117-126.
- Gale, N.H., Woodhead, A.P., Stos-Gale, Z.A., Walder, A. and Bowen, I., 1999. Natural variations detected in the isotopic composition of copper: possible applications to archaeology and geochemistry. *International Journal of Mass Spectrometry*, 184, pp.1-9. [http://dx.doi.org/10.1016/S1387-3806\(98\)14294-X](http://dx.doi.org/10.1016/S1387-3806(98)14294-X).
- Gibbs, G.V., Cox, D.F., Rosso, K.M., Ross, N.L., Downs, R.T. and Spackman, M.A., 2007. Theoretical electron density distributions for Fe- and Cu-sulfide earth materials: A connection between bond length, bond critical point properties, local energy densities, and bonded interactions. *Journal of Physical Chemistry B*, 111(8), pp.1923-1931. <http://dx.doi.org/10.1021/jp065086i>.
- Goh, S.W., Buckley, A.N., Lamb, R.N., Rosenberg, R.A. and Moran, D., 2006. The oxidation states of copper and iron in mineral sulfides, and the oxides formed on initial exposure of chalcopyrite and bornite to air. *Geochimica et Cosmochimica Acta*, 70(9), pp.2210-2228. <http://dx.doi.org/10.1016/j.gca.2006.02.007>.
- Goh, S.W., Buckley, A.N., Skinner, W.M. and Fan, L.J., 2010. An X-ray photoelectron and absorption spectroscopic investigation of the electronic structure of cubanite, CuFe<sub>2</sub>S<sub>3</sub>. *Physics and Chemistry of Minerals*, 37(6), pp.389-405. <http://dx.doi.org/10.1007/s00269-009-0341-z>.
- Goldenberg, G., Anfinset, N., Silvestri, E., Belgrado, E., Hanning, E.K., Klauzner, M., Schneider, P., Staudt, M. and Töchterle, U., 2011. Das Nepal-Experiment - experimentelle Archäometallurgie mit ethnoarchäologischem Ansatz. In: K. Oeggel, G. Goldenberg, M. Prast and T. Stöllner, eds. 2011. *Die Geschichte des Bergbaus in Tirol und seinen angrenzenden Gebieten*. Proceedings 5. Mile-

- stone-Meeting SFB HiMAT 7. - 10.10.2010 in Mühlbach. Innsbruck: Innsbruck University Press. pp.83-90.
- Gražulis, S., Chateigner, D., Downs, R.T., Yokochi, A.F.T., Quirós, M., Lutterotti, L., Manakova, E., Butkus, J., Moeck, P. and Le Bail, A., 2009. Crystallography Open Database - an open-access collection of crystal structures. *Journal of Applied Crystallography*, 42(4), pp.726-729. <http://dx.doi.org/10.1107/S0021889809016690>.
- Gražulis, S., Daškevič, A., Merkys, A., Chateigner, D., Lutterotti, L., Quirós, M., Serebryanaya, N.R., Moeck, P., Downs, R.T. and Le Bail, A., 2012. Crystallography Open Database (COD): An open-access collection of crystal structures and platform for world-wide collaboration. *Nucleic Acids Research*, 40 (Database issue), D420-7. <http://dx.doi.org/10.1093/nar/gkr900>.
- Hanning, E.K., 2012. Reconstructing Bronze Age copper smelting in the Alps: an ongoing process. *Experimentelle Archäologie in Europa*, 11, pp.75-86.
- Hanning, E.K. and Pils, R., 2011. Experimentelle Untersuchungen zur bronzezeitlichen Kupferverhüttung im ostalpinen Gebiet - Erste Ergebnisse. In: K. Oegg, G. Goldenberg, M. Prast and T. Stöllner, eds. 2011. *Die Geschichte des Bergbaus in Tirol und seinen angrenzenden Gebieten*. Proceedings 5. Milestone-Meeting SFB HiMAT 7. - 10.10.2010 in Mühlbach. Innsbruck: Innsbruck University Press. pp.129-134.
- Hanning, E.K., Herdits, H. and Silvestri, E., 2015. Alpines Kupferschmelzen – technologische Aspekte. In: T. Stöllner and K. Oegg, eds. 2015. *Bergauf bergab: 10.000 Jahre Bergbau in den Ostalpen*. Veröffentlichungen aus dem Deutschen Bergbau-Museum Bochum, 207. Bochum: Deutsches Bergbau-Museum, Rahden/Westfalen: Marie Leidorf. pp.225-231.
- Heiss, A.G. and Oegg, K., 2008. Analysis of the fuel wood used in Late Bronze Age and Early Iron Age copper mining sites of the Schwaz and Brixlegg area (Tyrol, Austria). *Vegetation History and Archaeobotany*, 17(2), pp.211-221. <http://dx.doi.org/10.1007/s00334-007-0096-8>.
- Hentze, E., 1929. *Sintern, Schmelzen und Verblasen sulfidischer Erze und Hüttenprodukte*. Berlin, Heidelberg: Springer.
- Herdits, H. and Löcker, K., 2004. Eine bronzezeitliche Kupferhütte im Mitterberger Kupferkies-Revier (Salzburg): Ausgrabung und Rekonstruktion. In: G. Weisgerber and G. Goldenberg, eds. 2004. *Alpenkupfer: Rame delle Alpi*. Veröffentlichungen aus dem Deutschen Bergbau-Museum, 122. Bochum: Deutsches Bergbau-Museum. pp.177-188.
- Jansen, M., 2018. On the use of Cu isotope signatures in archaeometallurgy: A comment on Powell et al., *Journal of Archaeological Science*, 93(5), pp.221-215. <http://dx.doi.org/10.1016/j.jas.2018.02.016>.
- Klein, S., 2007. Dem Euro der Römer auf der Spur - Bleiisotopenanalysen zur Bestimmung der Metallherkunft römischer Münzen. In: G.A. Wagner, ed. 2007. *Einführung in die Archäometrie*. Berlin: Springer. pp.139-152.
- Klein, S. and Rose, T., 2020. Evaluating copper isotope fractionation in the metallurgical operational chain: An experimental approach. *Archaeometry*, 62(S1), pp.134-155. <http://dx.doi.org/10.1111/arc.12564>.
- Klein, S., Brey, G.P., Durali-Müller, S. and Lahaye, Y., 2010. Characterisation of the raw metal sources used for the production of copper and copper-based objects with copper isotopes. *Archaeological and Anthropological Sciences*, 2(1), pp.45-56. <http://dx.doi.org/10.1007/s12520-010-0027-y>.
- Lechtman, H.N. and Klein, S., 1999. The Production of Copper-Arsenic Alloys (Arsenic Bronze) by Cosmelting: Modern Experiment, Ancient Practice. *Journal of Archaeological Science*, 26(5), pp.497-526. <http://dx.doi.org/10.1006/jasc.1998.0324>.
- León-Reina, L., García-Maté, M., Álvarez-Pinazo, G., Santacruz, I., Vallcorba, O., La Torre, A.G. de and Aranda, M.A.G., 2016. Accuracy in Rietveld quantitative phase analysis: A comparative study of strictly monochromatic Mo and Cu radiations. *Journal of Applied Crystallography*, 49(3), pp.722-735.
- Lindsley, D.H., 1967. Experimental Studies of Oxide Minerals. *Reviews in Mineralogy and Geochemistry*, 3, pp.61-88.
- Mathur, R. and Fantle, M.S., 2015. Copper Isotopic Perspectives on Supergene Processes: Implications for the Global Cu Cycle. *Elements*, 11(5), pp.323-329. <http://dx.doi.org/10.2113/gselements.11.5.323>.
- Matthes, W.E., 2018. *Keramische Glasuren: Ein Handbuch mit über 1100 Rezepten*. Mit Erläuterungen und Formeln. 6<sup>th</sup> edn. Koblenz: Hanusch.
- Mikhlin, Y., Tomashevich, Y., Tauson, V., Vyalikh, D., Molodtsov, S. and Szargan, R., 2005. A comparative X-ray absorption near-edge structure study of bornite, Cu<sub>5</sub>FeS<sub>4</sub>, and chalcopyrite, CuFeS<sub>2</sub>. *Journal of Electron Spectroscopy and Related Phenomena*, 142(1), pp.83-88. <http://dx.doi.org/10.1016/j.elspec.2004.09.003>.
- Moesta, H. and Schnau, G., 1983. Bronzezeitliche Hüttenprozesse in den Ostalpen: III. Die Abscheidung des metallischen Kupfers. *Naturwissenschaften*, 70, pp.142-143.
- Morgan, J.L., 1867. On the Smelting of Refractory Copper Ores with Wood as Fuel in Australia (Including Plate). *Minutes of the Proceedings of the Institution of Civil Engineers*, 26, pp.44-46. <http://dx.doi.org/10.1680/imotp.1867.23153>.
- Nelle, O. and Klemm, S., 2010. Wood and Charcoal Supplies for Prehistoric and Mediaeval Mining Activities in the Eisenerzer Ramsau, Styria, Austria. In: P. Anreiter, ed. 2010. *Mining in European history and its impact on environment and human societies: Proceedings for the 1<sup>st</sup> Mining in European History-Conference of the SFB-HIMAT, 12.-15. November 2009, Innsbruck*. Innsbruck: Innsbruck University Press. pp.177-182.
- Nickel, E.H., 1995. The Definition of a Mineral. *The Canadian Mineralogist*, 33, pp.689-690. Available at: <[http://rruff.info/doclib/cm/vol33/CM33\\_689.pdf](http://rruff.info/doclib/cm/vol33/CM33_689.pdf)> [Accessed: 4 November 2020].
- Pliny [1855] *Naturalis Historia (The natural history): Translated, with copious notes and illustrations, by the late John Bostock and H. T. Riley*. London: H. G. Bohn. Available at: <<https://catalog.perseus.org/catalog/urn:cts:latinLit:phi0978.phi001.perseus-engl>> [Accessed: 4 November 2020].
- Powell, W., Mathur, R., Bankoff, H.A., Mason, A., Bulatović, A., Filipović, V. and Godfrey, L., 2017. Digging deeper:



- Insights into metallurgical transitions in European prehistory through copper isotopes. *Journal of Archaeological Science*, 88, pp.37-46. <http://dx.doi.org/10.1016/j.jas.2017.06.012>.
- Powell, W., Mathur, R., Bankoff, A.H., John, J., Chvojka, O., Tisucká, M., Bulatović, A., Filipović, V., 2018. Copper isotopes as a means of determining regional metallurgical practices in European prehistory: A reply to Jansen. *Journal of Archaeological Science*, 93, pp.216-221. <http://dx.doi.org/10.1016/j.jas.2018.02.015>.
- Raghavan, V., 2004. Cu-Fe-S (Copper-Iron-Sulfur). *Journal of Phase Equilibria & Diffusion*, 25(5), pp.450-454. <http://dx.doi.org/10.1361/15477030420845>.
- Rose, T., Hanning, E.K. and Klein, S., 2019. Verhüttungsexperimente mit Chalkopyrit-Erz nach Vorbildern aus dem bronzezeitlichen Ostalpenraum und Nepal. *Experimentelle Archäologie in Europa*, 18, pp.47-60. <http://dx.doi.org/10.23689/figeo-3706>.
- Rose, T., Klein, S. and Hanning, E.K., 2020. Copper isotope fractionation during prehistoric smelting of copper sulfides: experimental and analytical data. *GFZ data services*. <http://dx.doi.org/10.5880/figeo.2020.013>.
- Rose, T., Morgenstern, G., Stelter, M. and Klein, S., 2017. Cu isotope fractionation during prehistoric smelting: a contribution of modern pyrometallurgy. In: *Proceedings of the European Metallurgical Conference 2017* (4 vols). Clausthal-Zellerfeld: GDMB. pp.1153-1167.
- Schibler, J., Breitenlechner, E., Deschler-Erb, S., Goldenberg, G., Hanke, K., Hiebel, G., Hüster Plogmann, H., Nicolussi, K., Marti-Grädel, E., Pichler, S., Schmidl, A., Schwarz, S., Stopp, B. and Oeggl, K., 2011. Miners and mining in the Late Bronze Age: A multidisciplinary study from Austria. *Antiquity*, 85(330), pp.1259-1278. <https://dx.doi.org/10.1017/S0003598X00062049>.
- Shamsuddin, M., 2016. *Physical Chemistry of Metallurgical Processes*. Berlin: Springer International Publishing.
- Stöllner, T., 2011. Der Mitterberg als Großproduzent für Kupfer in der Bronzezeit: Fragestellungen und bisherige Ergebnisse. In: K. Oeggl, G. Goldenberg, M. Prast and T. Stöllner, eds. 2011. *Die Geschichte des Bergbaus in Tirol und seinen angrenzenden Gebieten*. Proceedings 5. Milestone-Meeting SFB HiMAT 7. - 10.10.2010 in Mühlbach. Innsbruck: Innsbruck University Press. pp.93-106.
- Stöllner, T., Hanning, E.K. and Hornschuch, A., 2011. Ökonometrie des Kupferproduktionsprozesses am Mitterberger Hauptgang. In: K. Oeggl, G. Goldenberg, M. Prast and T. Stöllner, eds. 2011. *Die Geschichte des Bergbaus in Tirol und seinen angrenzenden Gebieten*. Proceedings 5. Milestone-Meeting SFB HiMAT 7. - 10.10.2010 in Mühlbach. Innsbruck: Innsbruck University Press. pp.115-128.
- Toby, B.H. and Dreele, R.B., 2013. GSAS-II: The genesis of a modern open-source all purpose crystallography software package. *Journal of Applied Crystallography*, 46(2), pp.544-549. <http://dx.doi.org/10.1107/S0021889813003531>.
- Töchterle, U., Goldenberg, G., Schneider, P. and Tropper, P., 2013. Spätbronzezeitliche Verhüttungsdüsen aus dem Bergbaurevier Mauken im Unterinntal, Nordtirol: Typologie, mineralogisch- petrographische Zusammen-  
setzung und experimentelle Rekonstruktionsversuche. *Der Anschnitt*, 65(1-2), pp.2-19.
- Tylecote, R.F., Ghaznavi, H.A. and Boydell, P.J., 1977. Partitioning of Trace Elements Between the Ores, Fluxes, Slags and Metal During the Smelting of Copper. *Journal of Archaeological Science*, 4, pp.305-333. [http://dx.doi.org/10.1016/0305-4403\(77\)90027-9](http://dx.doi.org/10.1016/0305-4403(77)90027-9).
- Zschocke, K. and Preuschen, E., 1932. *Das urzeitliche Bergbaugebiet von Mühlbach-Bischofshofen*. Wien: Anthropologische Gesellschaft.

## Authors

Thomas Rose (Corresponding author)  
Deutsches Bergbau-Museum Bochum  
Research Division Archaeometallurgy  
Am Bergbaumuseum 31  
44791 Bochum, Germany

Ben-Gurion University of the Negev  
Department of Bible  
Archaeology and Ancient Near East  
Be'er Sheva, Israel

Sapienza University of Rome  
Department of Antiquity  
Via dei Volsci 122, 00185 Rome, Italy  
Thomas.Rose@daad-alumni.de  
ORCID: 0000-0002-8186-3566

Erica Hanning  
RGZM Mainz  
Kompetenzbereich Experimentelle Archäologie  
An den Mühlsteinen 7  
56727 Mayen, Germany  
Hanning@rgzm.de

Sabine Klein  
Deutsches Bergbau-Museum Bochum  
Research Division Archaeometallurgy  
Am Bergbaumuseum 31  
44791 Bochum, Germany  
Sabine.Klein@bergbaumuseum.de  
ORCID: 0000-0002-3939-4428